Hydrogen in Enameling Steel

By ByeoungSoo Ahn

A thesis submitted to the Faculty of Graduate Studies and Research in partial fulfillment of the requirements for the degree of Master of Engineering.

Department of Mining and Metallurgical Engineering
McGill University, Montreal, Quebec, Canada
September 2000

ABSTRACT

Enameling steel, used in a vast range of applications, can suffer from a surface defect resembling fish scale. In this study, the effects of several microstructural, physical and coating factors on the hydrogen diffusion in low carbon steel were investigated using an electrochemical permeation apparatus, to find out the way to prevent the surface defects on the enamel coatings.

A new mechanism explaining the formation of the surface defects on the enameling steel was proposed after summarizing the experimental results. Then, the effects of porosity, dislocation density, the surface roughness of a steel substrate, oxide passive layer and Pd coating on the hydrogen diffusion coefficient, hydrogen concentration and hydrogen flux were investigated.

The variations of hydrogen diffusion coefficient, hydrogen concentration in steel and hydrogen flux caused by all factors listed previously were calculated in order to understand the effect of these factors on hydrogen diffusion.

RÉSUMÉ

L'acier émaillé, utilisé dans une vaste gamme d'applications, peut présenter des défauts en surface semblables à des écailles de poissons. Dans cette étude, les effets de plusieurs facteurs microstructuraux et physiques, sur la diffusion de l'hydrogène dans un acier à bas carbone ont été étudiés en utilisant un appareil de pénétration électrochimique, pour essayer de trouver le moyen d'empêcher la formation de défauts en surface sur les.

Après avoir analysé les résultats des expériences, un nouveau mécanisme expliquant la formation de défauts en surface sur l'acier émaillé a été proposé. Ensuite, les effets de la porosité, de la densité de dislocation, de la rugosité de la couche d'acier du substrat, de la couche d'oxyde de passivation, ainsi que le revêtement du Pd ont été analysés en terme de coefficient de diffusion d'hydrogène, de concentration d'hydrogène et de flux d'hydrogène.

Les variations du coefficient de diffusion de l'hydrogène , la concentration d'hydrogène dans l'acier , et le flux d'hydrogène ont été calculés dans le but de comprendre les effets précis de la diffusion d'hydrogène.

ACKNOWLEDGEMENT

I will never forget the scholarly support and constant encouragement of my supervisor, Prof. Jerzy A. Szpunar who has guided me almost two years to finish this thesis. I cannot express my gratitude too much for his advice.

I would like to express my appreciation to In-ho Jung for his advice and discussion on this work. I also express my gratitude to Dr. Sang-hyun Cho for his assistance.

Particularly, I would like to thank fellow researchers Mr. S. Poplawski, Mr. Y. Cao, Dr. R. Narayanan, Mr. J. Lin, Dr. H. Li, Mr. R. Hazhaikch for their help.

Korean friends' consistent friendship and timely help made me comfortable and gave me impetus to complete this research. So I gratefully express my acknowledgement to Jong-tae Park, Ki-tae Lee, Bae-kyun Kim, Jae-young Cho, Jae-hoon Oh, Jin-soo Kim, Hyoung-bae Kim, and Sung-mo Yang.

Most of all, I really feel thank to my family, especially my wife, son and daughter for their patience and affection.

TABLE OF CONTENTS

LIST OF FIGURES

LIST OF PHOTOS AND TABLES

CHAPTER I.

Introduction

Enameling steel is one of the most widely employed coating techniques used to prevent corrosion. In this process, the steel surface is covered by enamel, a noble material belonging to the family of glasses. The economic costs of corrosion in the United States of America alone have been estimated between $8 billion and $126 billion per year. A perhaps more realistic annual $30 billion has been suggested for the savings that could result if all economically useful measures were taken to prevent or minimize corrosion.[1] Enamel has excellent properties such as high resistance to corrosion, high temperatures failure, X-ray irradiation, and abrasion. Numerous colors of enamel are available. The enamel coatings are electrically insulating and graffiti-proof. Therefore, the process of enameling steel is used for a vast range of applications for domestic appliances, cooking utensils, architectural panels, special coating, etc.[1,2] In order to improve the properties of the coated steel, continuous casting methods are used to provide regular chemistry, homogeneous microstructures, and greater internal soundness. The preparation operations, consists of acid pickling and nickel plating, influence direct enameling.[3] The chemical homogeneity of steel composition and low inclusion content decrease the probability of formation of enameling defects such as black spots and hair-lines.

Enameling steel, however, produces a surface defect much like fish scale. The fish scale has the appearance of small chips or scales on the enameled surface,[4] as can be seen in Photo 1. Past studies have found that it is hydrogen that plays a major role in the formation of the fish scale. Enameling procedures have been well known to generate the

typical example of ingressing hydrogen. Near the temperature of firing enamel at 860°C, the hydrogen has high solubility and becomes supercharged during the cooling period. At ambient temperatures, hydrogen solubility in the steel substrate of enameling steel is very low and thus, the atomic hydrogen in the steel substrate is ejected from solution.[5,6,7] The atomic hydrogen may diffuse to the enamel-steel surface to form a molecular hydrogen gas, which builds up a gas pressure to cause a defect on the enameling surface. Actually, research has reported that the hydrogen in steel reacts with carbon to make methane above 200°C, causing swelling of the material and an eventual brittle-type failure.[1,8]

Therefore, the factors affecting hydrogen diffusion have been investigated to find out the way to reduce fish scale on the surface of enameling steel.[1,2] The effects of voids, vacancies, dislocations, grain boundaries and precipitates on hydrogen diffusion in steel were investigated to explain the hydrogen diffusion mechanism.[7,9-18] Nearly all metallic corrosion processes involve the transfer of electronic charge in aqueous solutions and the liberation of electrons that react with H^+ in solution to form H_2 molecules.[7] However, hydrogen diffusion is usually affected by the combination of several factors and is very sophisticated. Occasionally, investigations of the hydrogen diffusion in steel have been contradictory with each other.[9] Suffice is to say that the hydrogen diffusion mechanism is not well understood even until now.

In a first instance, this study proposes a new mechanism for the formation of surface defects in enameling steel, after careful observation of cracked enameling steel. Then, the effects of the presence of void area, passive layer, dislocation, Pd coating and surface roughness on hydrogen diffusion in low carbon steel were investigated by using a hydrogen permeation experiment.

(a)

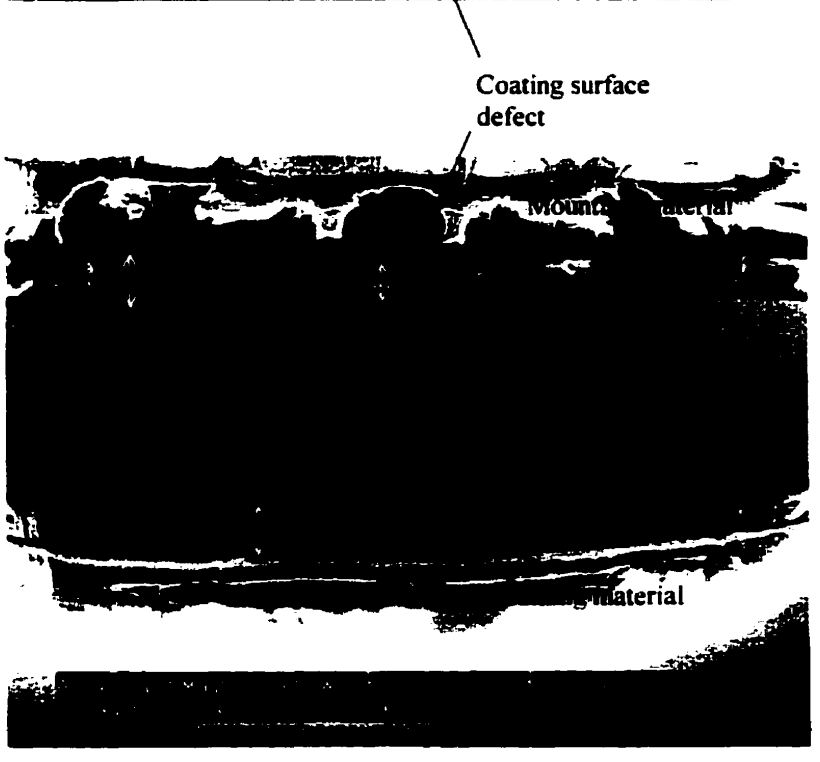

(b)

Photo 1. Fish scale defect of enameling steel surface as seen in a) an optical microscope b) a cross sectional SEM image

CHAPTER II.

Literature Review

2.1. Basic Theory of Metal-Hydrogen

2.1.1. General Description of Metal-Hydrogen Relation

Hydrogen is present everywhere from 7 or more miles below the earth crust to the upper limits of the atmosphere.[19] Therefore, metals often come into contact with hydrogen gas or hydrogen producing environments. Hydrogen has a unique ability to penetrate many solid metals directly from the gaseous state or from electrolytic processes because the hydrogen atom is very small and diffuses easily. Generally, hydrogen diffuses fast compared to oxygen and nitrogen in metals.[6] Hydrogen dissolves in the metal lattice, presented as a screened proton where its valence electron joins the electron cloud of the metal.[10]

Hydrogen atoms in the lattice of a metal causes metal degradation known as hydrogen embrittlement and, as a result, possibly disastrous failures in service structure materials.[3,6] Moreover, hydrogen embrittlement can occur in the presence of an applied stress without any build-up of high pressures in microcracks or at inclusion-metal interfaces. If large amounts of hydrogen are absorbed, there may be a general loss in ductility. Internal bursts or blisters may be realized if large amounts of hydrogen collect in localized areas. Small amounts of dissolved hydrogen may also react with microstructural features of alloys to produce catastrophic failures at applied stresses far below the yield strength.

All of the just described phenomena are collectively referred to as the hydrogen embrittlement. Hydrogen degradation of structural materials is considered a serious problem and has received much attention, since it may result in corrosion-related failures.[18,19]

2.1.2. Solubility of Hydrogen in Metals

The effects of atomic hydrogen depend upon the solubility of hydrogen in metals.[3,6,18,19] A classification system based on the metals' reaction with hydrogen yields three different classes. 'A' class metals are in 1~2 groups, 'B' class metals are in 12~18 groups, and 'C' class metals are in 3~11 groups, these are shown in Figure 1. Characteristic saline hydrides are formed between 'A' class metals and hydrogen, resulting in marked contraction, whereas gaseous metal hydrides compounds analogous to hydrocarbon are formed in 'B' class metals. 'A' and 'B' class metals do not occlude hydrogen through these reactions. 'C' class metals, however, exhibit somewhat diffusive occlusion of hydrogen. 'C' class metals are subdivided into two types; endothermic and exothermic occluders. Table 1 shows the characteristics of 'C' class metals.

The effect of atomic hydrogen on mechanical properties of a given metal or alloy will depend upon the hydrogen-metal system in question, especially on the solubility of hydrogen. Endothermic occluders such as Fe, Pt, Ni, Co, Cu, Al, and Ag form solid solutions with hydrogen. The solubility of hydrogen of these metals changes as the square root of the pressure according to Sievert's law. Metals take up small or moderate quantities of hydrogen at low temperature but dissolve more hydrogen as the temperature increases due to the characteristics of negative heat absorption. This is the characteristic of an endothermic occluder. The changes of gross dimensions brought about by absorption of hydrogen are too small to observe with certainty in these metals. Contrary to this, exothermic occluders such as Ti, Zr, V, Th, and Pd usually form compounds with the hydrogen, called 'hydride'. Exothermic metals take up larger quantities of hydrogen because of the positive heat reaction according to absorption, and the solubility decreases as the temperature increases. The hydrogen atoms in exothermic occluders are believed not to be completely ionized and are much larger than protons so their presence in

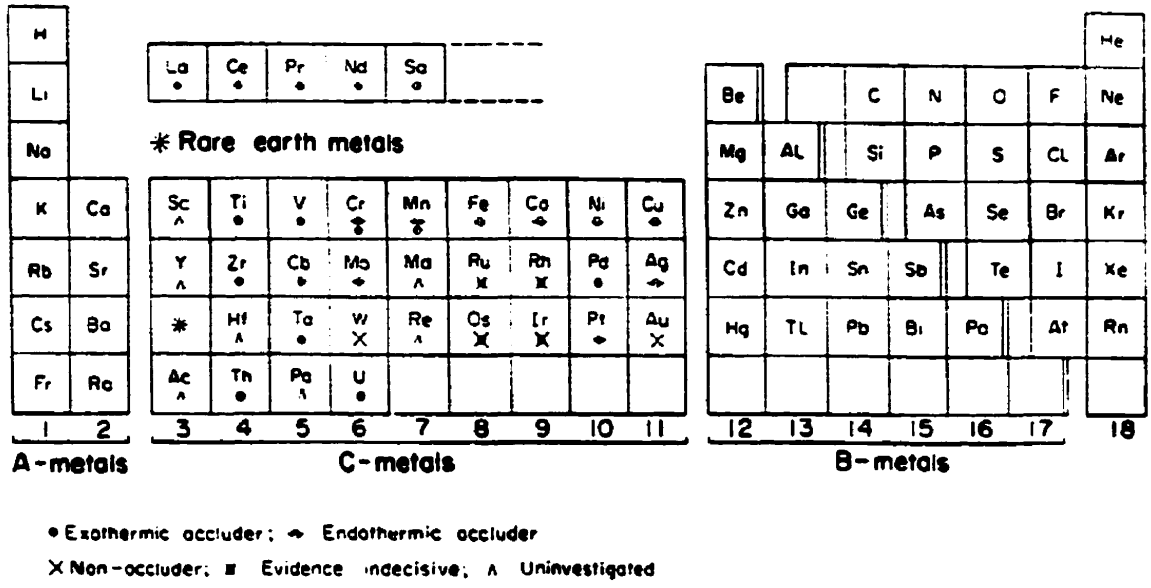

Figure 1. Metal-Hydrogen relationship[6]

Table 1. Two types of C class metals

Type	Endothermic occluder	Exothermic occluder
Element	Fe, Pt, Ni, Co, Cu, Ag	Ti, Zr, V, Th, Pd
M-H formation	Solid solutions	Compounds hydride
Heat of absorption	Negative - at low T, small quantities H - at high T, dissolve more H	Positive - at low T, large quantities H - at high T, solubility decrease
Dimension change	Too small to identify	10-15 % volume increase
H dissolving type in the metal lattice	- screened proton - valence electron joins the electron cloud of the metal	- not completely ionized - much larger than proton

interstitial positions tends to distort the lattice resulting in a volume increase of 10~15%. It is to note that the solubility here is measured at a state of equilibrium and determined for a given metal-hydrogen system solely by the external variables of temperature and pressure. Occlusive capacity depends on an additional variable - the degree of strain or condition of the metal with regard to plastic deformation.[19]

2.1.3. Hydrogen in Steels

In 1864, Cailletet discovered that small amounts of hydrogen were liberated when an iron specimen was immersed in dilute sulfuric acid and that hydrogen was absorbed by the metal.[20] In 1922, Bodenstein found that the quantity of atomic hydrogen entering iron could be varied by the application of a cathodic current.[21] From these observations. one could identify those hydrogen atoms produced electrochemically that may enter the metallic lattice and permeate through the metal.[3] Penetrative ability of hydrogen is much enhanced by the reaction of ionization or dissociation to atoms. Since the establishment of the theory of hydrogen permeation method using the electrochemical cell by Devanathan and Stachurski on palladium in 1962, there have been many researches about hydrogen in steels.[7,17,22-30] The electrochemical permeation method has been widely used to study hydrogen diffusion parameters in metals and particularly the hydrogen trapping in steels.[5,10-13,15,31] The method consists of creating a hydrogen concentration gradient in a metallic sample to achieve hydrogen diffusion through the metal sheet. The experimental results on steels have been scattered and the opinions on several phenomena observed are often in contradiction.[9] Table 2 shows the various hydrogen diffusion coefficients obtained from a number of experimental results. Moreover, a number of details in the mechanism of hydrogen diffusion and in the behavior of desorption in this system have not been fully understood.

Table 2. Diffusion coefficients of hydrogen in iron and mild steel[9,32]

$D=D_o\exp(-Q/RT)$ cm^2s^{-1}	$D25^oC$ (cm^2s^{-1})	Material	Source
$7.6\times10^{-4}\exp(-2280/RT)$	1.5×10^{-5}	iron	Sykes, Burton and Gegg
$2.2\times10^{-3}\exp(-2290/RT)$	1.4×10^{-5}	iron	Geller and Sun
$8.8\times10^{-4}\exp(-3050/RT)$	4.2×10^{-6}	iron	Stross and Tompkins
$9.3\times10^{-4}\exp(-2700/RT)$	8.2×10^{-6}	iron	Eichenauer, Kunzig and Pebler
$2.1\times10^{-3}\exp(-3300/RT)$	6.4×10^{-6}	mild steel	Smialowski
$5.3\times10^{-3}\exp(-3400/RT)$	5.0×10^{-6}	mild steel	Frank, Swets and Fry
$1.4\times10^{-3}\exp(-3200/RT)$	4.4×10^{-6}	iron	Johnston and Hill
$1.2\times10^{-1}\exp(-7820/RT)$	2.2×10^{-7}	iron	Johnston and Hill
$1.42\times10^{-3}\exp(-3270/RT)$	4.6×10^{-6}	iron	Wagner and Sizman
$1.1\times10^{-2}\exp(-3610/RT)$	2.5×10^{-5}	iron	Wach, Miodowinik and Mackowiak
-	2×10^{-6}	mild steel	Schuetz and Robertson
-	3×10^{-7}	mild steel	Palczewska and Ratajczyk
-	2×10^{-6}	mild steel	Palczewska and Ratajczyk
-	1×10^{-5}	iron	Raczynski
-	1.39×10^{-8}	iron	Alikin
-	8.3×10^{-5}	iron	Devanathan, Stachurski and Beck
-	5×10^{-6}	mild steel	Eschbach, Gross and Schlien
-	2.9×10^{-6}	iron	Veysseyre, Azou and Bastien
-	2.3×10^{-8}	mild steel	Davis

2.2. Hydrogen Permeability

Hydrogen permeation experiments have been frequently undertaken to investigate hydrogen diffusion in steel. Because this study also adopted this method, it is necessary to first of all understand this experiment in order to interpret the experimental results.

2.2.1. Electrochemical Reaction Theory[3,28]

The sources of electrolytic hydrogen in metals are many. Hydrogen can be introduced during cleaning, pickling, electroplating processes, or it may be picked up from the service environment as a result of cathodic protection or corrosion reactions. There is an unavoidable electrode reaction proceeding simultaneously with these processes whereby there is a discharge of hydrogen ions or water molecules:[1]

$$2H^+ + 2e^- \rightarrow H_2$$
$$2H_2O + 2e^- \rightarrow H_2 + 2OH^-$$

The reaction then produces hydrogen in acidic solutions electrolytically. In alkaline solutions, the breakdown of water produces hydrogen atoms and hydroxyl ions.

On passage of a current across a metal–electrolyte interface, the equilibrium potential difference at the interface is usually changed and the electrode becomes polarized. Polarization represents a change in potential with net current flow and an exchange current density that is exceeded. This overpotential is a deviation from the reversible (equilibrium) potential. With polarization, the efficiency of energy conversion (chemical to electrical) is a function of the current density. Overpotential is a necessary concomitant to the passage of a net current density across any interface. Reactions differ only in the magnitude of overpotential associated with a particular current density. For hydrogen overpotential, there could be a high or low overpotential, which indicates the difficulty or ease in the kinetics of the hydrogen evolution. For hydrogen embrittlement, it is important to look at the electrode kinetics of the hydrogen evolution reaction and see how the reaction can lead to hydrogen entry into metal. There are three mechanisms in the hydrogen evolution reaction.

$$H^+ + e + M \rightarrow (M\text{-}H)\ ;\ \text{electrochemical discharge}$$
$$(M\text{-}H) + (M\text{-}H) \rightarrow 2M + H_2\uparrow\ ;\ \text{recombination}$$
$$(M\text{-}H) + H^+ + e \rightarrow M + H_2\uparrow\ ;\ \text{electrochemical desorption}$$

After the electrochemical discharge step, the newly formed hydrogen atoms are adsorbed on the surface. The majority of these hydrogen atoms combine to form hydrogen molecules and harmlessly form bubbles of hydrogen gas. Usually only a small portion of the hydrogen liberated at the cathode enters into the metal. It is precisely these atoms of hydrogen that cause embrittlement of metal. Hydrogen can permeate through the metallic surface by two paths:

$$2H^+ + 2e \rightarrow 2H^0_{ads} \rightarrow H_2\ ;\ \text{recombination reaction}$$
$$H^+ + e \rightarrow H_{ads} + H^+ + e \rightarrow H_2\ ;\ \text{catalytic recombination}$$

In acidic solutions, hydrogen ions are reduced to form neutral hydrogen atoms. The discharge reaction will not proceed unless hydrogen ions are available. Water is an ever present source of hydrogen. In alkaline solutions, there is a reduction of water molecules. The discharge of water molecules also yields adsorbed hydrogen atoms. The surface adsorption of atomic hydrogen on the metallic substrate is important in the diffusion process. Some fraction of hydrogen may permeate into the metal. It is this small fraction of hydrogen after entering the metal lattice that causes insidious embrittlement phenomenon in metals. Hydrogen coverage on a metal and the variation of that coverage with potential is of considerable importance in assessing the rate of entry of hydrogen into a metal during cathodic polarization. The surface metal oxides tend to act as barriers to hydrogen entry.

2.2.2. Entry of Electrolytic Hydrogen into Metals

A number of metals can absorb hydrogen, and this absorption provides an alternative reaction path to the chemical or electrochemical desorption of hydrogen atoms. Usually only a small portion of the hydrogen liberated at the cathode enters into the metal. The rate of hydrogen entry depends on many variables: the nature of the metal or alloy, its composition and thermal-mechanical history, surface conditions, composition of the electrolyte, cathodic current density, electrode potential, temperature, pressure, etc. Most of the kinetics of hydrogen at the entry and exit side of metal have been studied by permeating hydrogen through a thin metal specimen as shown in Figure 2.[28] At steady state, the flux of hydrogen is

$$J_\infty = \frac{D(C_0 - C_L)}{L} \qquad (2.1)$$

where D is the diffusion coefficient, L is the thickness of the membrane, C_0 is the subsurface concentration of hydrogen at the entry side, and C_L is the concentration of hydrogen just below the exit side.

The hydrogen diffusing out at the exit side of the membrane is electrochemically oxidized by maintaining a constant anodic potential using a potentiostat. The anodic current density provides a direct measure of the hydrogen flux ($i_p = zFJ$). The electrolyte used at the exit side of the membrane is alkaline, usually 0.1 N NaOH solution. The concentration C_L is zero owing to the rapid removal of the hydrogen diffused through and the entry concentration C_0 governs the magnitude of the concentration gradient. The measured rate of permeation expresses the net rate of hydrogen entry if D and L values are constant. Therefore the electrochemical method is very convenient for studying the effect of environmental factors on hydrogen entry. After hydrogen is absorbed, it goes into the dissolved state by jumping into the interstitial spaces beneath the first atomic layer. From this dissolved state, hydrogen diffuses into the bulk and its rate is proportional to hydrogen coverage at the surface. Dissolved hydrogen usually remains in

the interstitial spaces available in the lattice. The diffusion of hydrogen in the metal is the slowest step in the permeation process.

2.2.3. Typical Hydrogen Permeation Curve

Typical transient record of hydrogen permeation is shown in Figure 3.[22,24] From the anodic current change, the hydrogen permeation curve can be obtained schematically like this figure.

As the time flows the hydrogen permeation current is recorded. '$i_{A\infty}$' represents the steady state current. The diffusion coefficient can be calculated by the time lag method and the breakthrough time method. Starting from zero time, the breakthrough time that is represented by 'T_b' in this figure is the start time of anodic current at the exit side. It is defined as the time between the increase of cathodic current at the entry side and the onset of the anodic current at the exit side. Time lag, 'T_L', is the time required for the permeation to reach 0.63 times the steady state value. 'T_L' is the intercept on the time axis of the straight line in the time integral of permeation current. From this value of the time lag, the diffusion constant can be obtained from the following equation:[22]

$$T_L = L^2/6D \qquad (2.2)$$

where L is the thickness of the specimen and D is the diffusion constant.

2.3. Factors Affecting Hydrogen Diffusion in Steel

Hydrogen diffusing through a metal lattice accumulates at metallurgical inhomogeneities or traps.[10-12] The accumulation causes a lag in the hydrogen flux through a sheet specimen. Figure 4 shows the effect of such traps.[1,10] The difference between consecutive transients shows that hydrogen penetrates in a much shorter time after the traps have been filled. The rate of steady state hydrogen diffusion is reduced by the presence of traps indicating that these traps have an attraction for the passing hydrogen flux. Traps may result from solute atoms, dislocations, particle-matrix

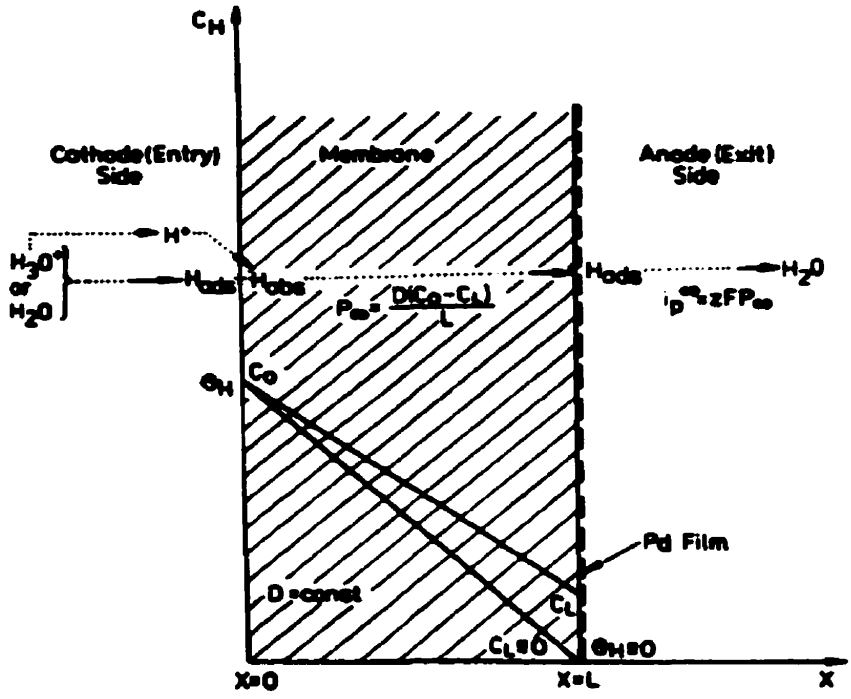

Figure 2. Permeation of electrolytic hydrogen through a metal membrane[28]

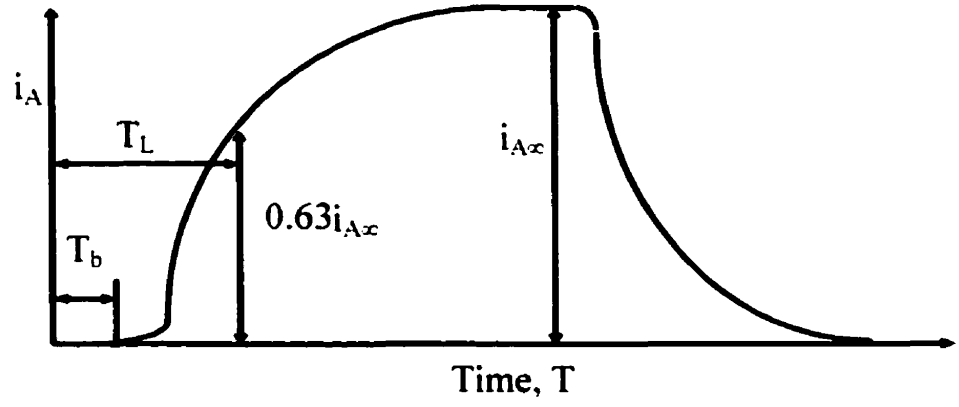

Figure 3. Typical hydrogen permeation curve[22,24]

interfaces, grain boundaries, and internal voids and cracks. Traps may be reversible or irreversible depending on whether the trapped hydrogen is easily released or tightly bound.

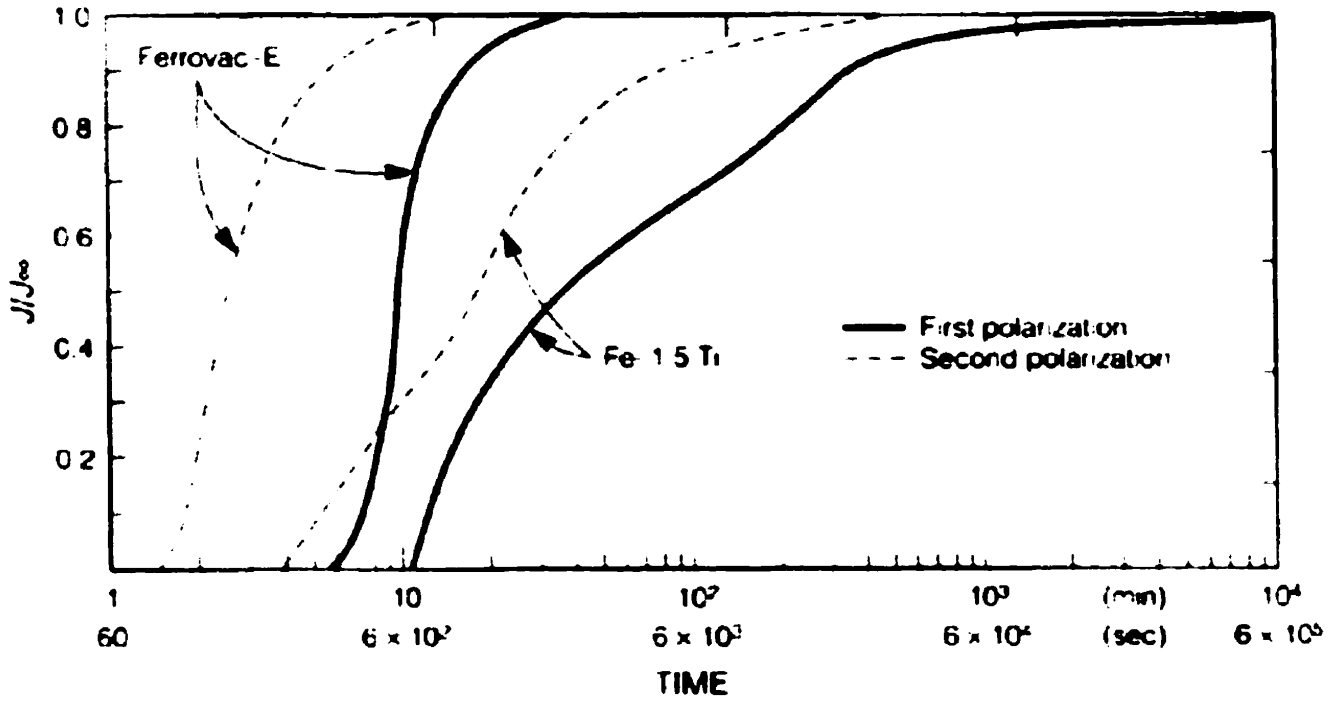

Figure 4. Hydrogen transients through iron and iron-titanium sheet[1.10]

Table 3 shows the classification and interaction energy of traps. The traps may be mobile like dislocations or stationary like grain boundaries and particles. Hydrogen diffusion in steel depends on both internal and external factors of the steel substrate. Many investigations have been done to find the effect of each factor on the hydrogen diffusion in steel.[6,9,10,12,13,24,27,32,33]

Table 3. Classification of hydrogen traps in steels[35]

Trap class	Example of trap: Elements at the left of iron	Example of trap: Elements with a negative ε'_H (b)	Interaction energy(a), eV	Character if known	Influence diameter, D_t
Point	...	Ni	(0.083)	Most probably Reversible	A few interatomic spacings
	Mn	Mn	(0.09)		
	Cr	Cr	(0.10)		
	V	V	(0.16)		
	...	Ce	(0.16)		
	...	Nb	(0.16)		
	Ti	Ti (vacancy)	0.27	Reversible	
	Sc	O	(0.71)		
	Ca	Ta	(0.98)		
	K	Ia	(0.98)	Getting more irreversible	
	...	Nd	(1.34)		
Linear	Dislocations		0.31 0.25 (average values)	Reversible Reversible	3nm for an edge dislocation
	Intersection of three grain boundaries		...	Depends on coherency	...
Planar or bimensional	Particle/matrix interfaces				
	TiC(incoherent)		0.98	Irreversible, gets more reversible as the particle is more coherent	Diameter of the particle, or a little more as coherency increases
	Fe3C		0.8~0.98		
	MnS				
	Grain boundaries		0.27 Average value 0.55~0.61(high angle)	Reversible Reversible or irreversible	Same as dislocation
	Twins		...	Reversible	A few interatomic spacings
	Internal surfaces(voids)		...	...	...
Volume	Voids		>0.22	...	Dimension of the defect
	Cracks		...	...	
	Particles		Depends on exothermicity of the dissolution of H by the particle	...	

(a) Values of interaction energies are either experimental or are calculated (when between parentheses) at room temperature (b) ε'_H is the interaction coefficient. A negative ε'_H means hydrogen is attracted.

2.3.1. Microvoids

Microvoids existing at non-metallic inclusions hamper desorption of hydrogen from mild steel and free–cutting steel. Evans and Rollason found a correlation between the volume of microvoids introduced by cold working and the effective diffusion coefficient of hydrogen in experimental low carbon steel.[36] They showed that trapping was reversible because all trapped hydrogen desorbed at room temperature. The voids are unsaturable, the amount of hydrogen trapped in them increasing without limit with increasing hydrogen activity.

Assuming equilibrium between hydrogen in voids and in metal, Ellerbrock et al. derived the following equation for the effective diffusion coefficient of hydrogen in a metal containing micropores:[11,34]

$$D_{eff} = D\{1 + \frac{4VMep_0 fC}{RTc_0^2} \exp(2\Delta H / RT)\}^{-1} \qquad (2.3)$$

where p_0 and c_0 are constants, f is the concentration of micropores, and $\square H$ is the enthalpy of solution of hydrogen in the metal. The above equation was derived under the assumption that the equilibrium between the hydrogen contained in pores, treated as an ideal gas, and that in metal can be described by Sievert's law. The equation shows that the influence of pores is more pronounced at lower temperatures and higher porosities. This is in good agreement with the experimental results usually obtained for cold deformed steel and iron. The equation, however, can predict another parameter profile in contrast with the experiment. The effective diffusion coefficient should decrease with increasing hydrogen concentration according to the equation. This is the consequence of the fraction of trapped hydrogen increasing with hydrogen pressure by Sievert's law. But the results from the deformed iron usually show a reverse trend, D_{eff} becoming higher at higher hydrogen concentrations. Therefore, the fixed numbers of voids are not the dominating traps in pure, cold deformed iron. If the voids' density or size increased with increasing cold work, the voids could show that result. After heating and quenching, the hydrogen in pure iron presents itself in the form of molecular gas. Both the desorption into a void and reabsorption by the metal proceed through a surface step which is not

very rapid at room temperature even for atomically clean surfaces. Moreover, many substances co-adsorbed with hydrogen on the metal surface can reduce rates of both adsorption and absorption. In the case of small voids, adsorption is the prevailing form of trapping because of the high surface-to-volume ratio.

2.3.2. Vacancies

The interaction between vacancies and hydrogen has been studied theoretically. Bakes et al. considered a cluster of about 40 atoms arranged in a bcc lattice containing a vacancy and a hydrogen atom.[15] They found that hydrogen is located 0.096 nm off the vacancy center along the <100> axis, which is in good agreement with the experimental data. Particle and ion irradiation methods are the most effective ways to obtain vacancy-rich materials, but dislocations are also present in considerable numbers. It is very difficult to obtain the predominant vacancy defect, so the works on hydrogen trapping by vacancies are few. The interaction energy observed in quenched iron by vacancy trapping was estimated 48.6 kJ/mol, and 59kJ/mol in high purity deformed iron.

2.3.3. Dislocations

Cold deformation of iron and steels results in a drop of diffusion coefficient by up to three orders of magnitude. The presence of dislocations is in a large degree responsible for a catastrophic drop of hydrogen diffusion coefficient in iron around room temperature.

From the early results of both internal friction and permeation measurements, the energy of dislocation trapping was 27 kJ/mol.[15] Recent experiments performed at low hydrogen concentrations in the order of 10^{-6} at.% showed that the binding energy was 49 to 58 kJ/mol, and was independent of temperature and amount of cold work.[12,17,37] In pure iron, however, dislocation trapping has not been observed by autoradiography. This is consistent with theoretical estimates showing that traps equilibrate with the lattice rapidly.[38] and with the fact that recent work did not find any deviations from equilibrium. Trapping on dislocations and dislocation boundaries has been observed in Fe-0.15% C alloy by tritium autoradiography.[15] Hydrogen trapping on dislocations was accompanied

by carbon segregation, and hydrogen seemed to be bound by segregated carbon rather than by the dislocation itself.

The effect of cold work on hydrogen trapping in steels is complex. In addition to increasing dislocation density, it can also create other trapping sites like microvoids and cracks, increase the boundaries of inclusions, and change their coherency with the matrix. Additionally, new traps can be produced by hydrogen if charging is performed at high fugacities, which normally is the case when electrochemical permeation measurements are performed. This results in complex behavior, such as the appearance of maximum on permeation-time curves and non-monotonic dependence of permeation on input hydrogen concentration.[15]

2.3.4. Interfacial Surfaces

The energy of hydrogen adsorption on an atomically clean iron surface depends on the degree of coverage, ranging from 130 kJ/mol for $\theta = 0$ to about 60 kJ/mol for $\theta = 1$. Here, θ is the fractional occupancy of surface sites. These values are equivalent to trapping energies of 100 to 30 kJ/mol.[15]

In steels, hydrogen can be trapped by the surfaces of voids, cracks, and incoherent inclusions. In complex materials such as steels, the surface composition may differ from that of the metal bulk because of the segregation of components, which may be of equilibrium segregation or kinetic origins. In a Fe-15%Cr alloy, drastic surface enrichment was observed, where the surface layer contained up to 60% Cr. Impurities co-adsorbed with hydrogen, known as catalytic poisons, change the adsorption energy and lower the rates of hydrogen recombination and H_2 dissociation. [15]

2.3.5. Grain Boundaries

In pure iron, grain boundary trapping has not been observed by either autoradiography or by the diffusion technique, where diffusivities were found to be independent of grain size.[39] Estimates based on the analogy of an atomic picture of grain boundaries to that of edge dislocation cores give 59 kJ/mol for trapping energy. A number of impurities were

found to segregate to the grain boundaries, including S, P, Sb, Sn, and C. Preliminary experiments show that P and Sb do not increase trapping ability of grain boundaries in Ni-Cr steel. Sulfur in the concentration range from 5 to 160 ppm has been found to exert a very small effect on the diffusion of hydrogen in iron. The effect of carbon on grain boundary segregation has been investigated. Combined techniques of ^{14}C and tritium autoradiography show that hydrogen is trapped at the grain boundaries only when they are decorated with carbon or its precipitates. Similar effects are found in a Fe-9%Cr and Fe-Ti alloys, and Armco iron.[15]

2.3.6. Microstructure

The effect of thermal treatment and resulting microstructure on the transport of hydrogen in steels has been investigated, but the conclusions regarding trapping are somewhat speculative, because the experimental methods employed do not allow identification of sites of hydrogen accumulation. According to the results of the influence of microstructure on hydrogen trapping in plain-carbon and low alloy steel by Asaoka et al., the most common traps were prior austenite grain boundaries and interfaces of lath martensite in quenched specimens.[15] Tempered specimens showed hydrogen segregation mainly at inclusions of MnS and spherical precipitates. In ferritic steels and alloys containing carbon, the accumulation of hydrogen at dislocations, grain boundaries, and matrix-precipitate interfaces appears to be affected by the presence and morphology of segregates and precipitates containing carbon. In austenitic steels, the trapping energies are generally lower than bcc iron based alloys. The trapping sites are ε-martensites, α-martensites, δ-ferrites, and inclusions of MnS. Trapping at the grain boundaries was chiefly related to the piling up of dislocations in these regions.[15]

2.3.7. Palladium Coating

Palladium coatings are widely used on metallic samples in which the hydrogen diffusion is to be measured at room temperature by means of the gas phase or electrochemical permeation techniques.[22-24,32] Surface effects may affect the diffusion measurements, especially near room temperature, in materials where the diffusion coefficient of hydrogen is large. The presence on both sides of the permeation samples

of a thin oxide layer grown in air or of a passive film built in alkaline solutions may be at the origin of the small values of the diffusion coefficient in iron and steels.[28,31,33,41-43] Palladium deposits on the detection side of the permeation samples are usually considered to be a way to prevent the metal from anodic dissolution in alkaline solutions. The usual palladium coating procedures are supposed to avoid the presence of oxide films on the metal. A few tens of nanometers thick layer of palladium on the entrance or exit side of the permeation samples should suppress all the oxide related problems on the diffusion measurement of hydrogen. Such problems include a decrease in the dissociation rate of the hydrogen molecule in gaseous hydrogen, time-dependent boundary conditions occurs in aqueous media due to changes in the oxide thickness and structure, a barrier effect due to a small diffusion coefficient or small solubility of hydrogen in the oxide, etc. The characteristics of the palladium/metal interface are not known and possible hydrogen trapping effects, due to incomplete elimination of the oxide during deposit, are neglected.

The palladium coating can also be deposited in ultra high vacuum devices by PVD method, in which case the pre-existing oxide can be removed before palladium deposition takes place by ion beam sputtering. The ion bombardment, however, may create structural defects at the metal surface. A thin layer of palladium is not supposed to alter the diffusion process of hydrogen due to the large value of the hydrogen diffusion coefficient in palladium. Nevertheless, the absorption, desorption and trapping of hydrogen in coated samples may be influenced by the palladium coating properties which depend on the deposition procedure. Furthermore, the influence of an oxide layer at the palladium-metal interface on the hydrogen concentration in coated samples has never been investigated.

CHAPTER III.

Experimental Procedure

3.1. Material

The material used in this project was the steel substrate for enameling. The thickness of the steel sheets was 1.10±0.05mm. In order to improve the properties of the steel/enamel combination, continuous casting method is used to provide more regular chemistries, homogeneous microstructures, and greater internal soundness. A 0.1% carbon content liquid steel bath is hot rolled and coiled above the eutectoid temperature, and then cold rolled heavily to create voids. The cold rolled steel should be decarburized in an open coil anneal furnace in order to reduce carbon levels to approximately 0.001%. Atomic emission spectrophotometry was used to evaluate the chemical composition of the steel substrate. Analyzed chemical composition of the substrate is given in Table 4.

3.2. Electrochemical Hydrogen Permeation

Electrochemical hydrogen permeation procedures are continuously being developed since 1962 when Devanathan and Stachurski proposed the electrochemical cell method for permeation measurements.[22,24] This technique uses anodic potentiostatic circuit currents, which maintains zero coverage on one side of the membrane, and, with the help of Faraday's laws, a direct measure of the instantaneous rate of permeation of hydrogen could be obtained.

The specimens used in this permeation test were cut from the steel plate shown in Figure 11. The permeation test was carried out twice on each specimen to get the reproducibility.

The schematic diagram of equipment of hydrogen permeation is shown in Figure 5. The specific procedure of this investigation is following. Electrochemical cell and O-rings were cleaned and dried completely. Graphite was used as an anode and Ni/NiO_2 as a cathode. The test specimen was clamped between the anodic (right side of Figure 5) and cathodic (left side of Figure 5) units; O-rings were used to ensure a constant area and airtight seal. A 90ml solutions of 0.1 N NaOH of were used as electrolyte on both sides. An electrical circuit was connected to the anodic and cathodic side to charge the sample. The passivation time was twelve hours long to ensure the hydrogen concentration level became negligible at the exit side. During passivation, the nitrogen gas was bubbled into both sides to remove oxygen and to get a homogeneous solution. A Ni/NiO_2 electrode was able to maintain a zero concentration of hydrogen on the exit side and to measure hydrogen to the parts per billion. After passivation, the current for hydrogen permeation was supplied to the cathode circuit potentiostatically to permeate hydrogen. The anode side of the cell was connected to the data recording system to measure the voltage change between the sample and the Ni/NiO_2 electrode. After a 100,000 seconds hydrogen permeation, the charging current was stopped and decayed.

The experimental conditions are summarized below:

Permeation surface area : 1.33 cm^2

Cathodic and anodic solution : 0.1 N NaOH

Cathodic charging current density : 1 $mAcm^{-2}$

Temperature : 21 ± 1.0 °C

3.3. Microscopic Observation

To check the voids, area and microstructure, an image analyzer and an optical microscope were used. The sample was ground and polished step by step. The final polish was accomplished using a 0.05 μm silica colloidal solution. After each step, the sample was cleaned using an ultrasonic cleaning apparatus with acetone. A solution of 3 % Nital was used to etch the polished sample to investigate the voids and the microstructure. The LECO 2005 image analyzer evaluated the void area and grain size

Table 4. Chemical composition of the enameling steel substrate

Element	C	Mn	P	S	Si	Cu	Mo
w/t(%)	0.007	0.226	0.041	0.028	<0.001	0.020	0.046

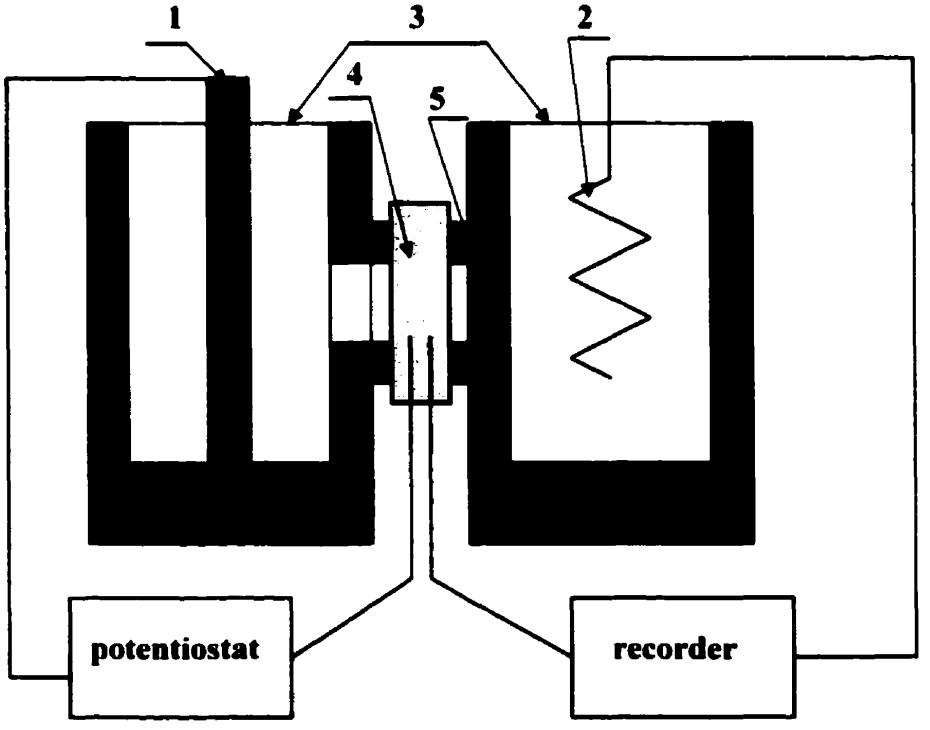

Figure 5. Schematic diagram of electrochemical cell

(1: cathode 2: anode 3: electrolytic cell 4: sample 5: O ring)

at a magnification of 1000X. The microstructure was examined by an optical microscope at a magnification of 1000X as well.

An X-ray diffractometer (Rigaku RU200BH, Siemens D500/D501) and an FEG-SEM (Philips XL30 . TSL OIM) were used to analyze the texture in the substrate layer and the enamel coating layer structure.

To check the cause of the fish scale of the enameling steel, the defect area of the enamel coated surface was cross sectioned and investigated.

3.4. Palladium Sputtering

Palladium sputtering was carried out by a plasma sputtering apparatus (Hummer VI) using a palladium target. The vacuum was 60~65 milli-torr. purged by argon gas during the plasma coating. The sputtering time was 3~8 minutes long as proposed by the reference manual to get the appropriate palladium thickness at a DC of 10 mA. Palladium coating was applied to the exit side of the sample only.

CHAPTER IV.

Experimental Results and Discussion

4.1. Texture of Steel Substrate

Generally, the texture of the material developed by the manufacturing process and the anisotropic microstructure affects all the microscopic and macroscopic properties of the material. The 'Orientation Distribution Function' (ODF) diagram of the enameling steel substrate is shown in Figure 6.

The ODF figure of the sample by the X-ray diffractometer shown in Figure 6 revealed that the sample has a typical rolling texture. The texture of the sample is described by γ fibers. It is evident that the steel substrate was heat treated after cold rolling. Figure 7 is the microstructure examined by the 'Orientation Imaging Microscope' (OIM). Here, the recrystallized grains, a result of decarburizing heat treatment, can be identified again in the pole figure.

4.2. Enamel Coating

4.2.1. The Permeability of Hydrogen through Enamel Coating

To learn more about the hydrogen diffusing through an enamel coating layer, the experiment of hydrogen permeation on the steel coated by enamel was performed. Figure

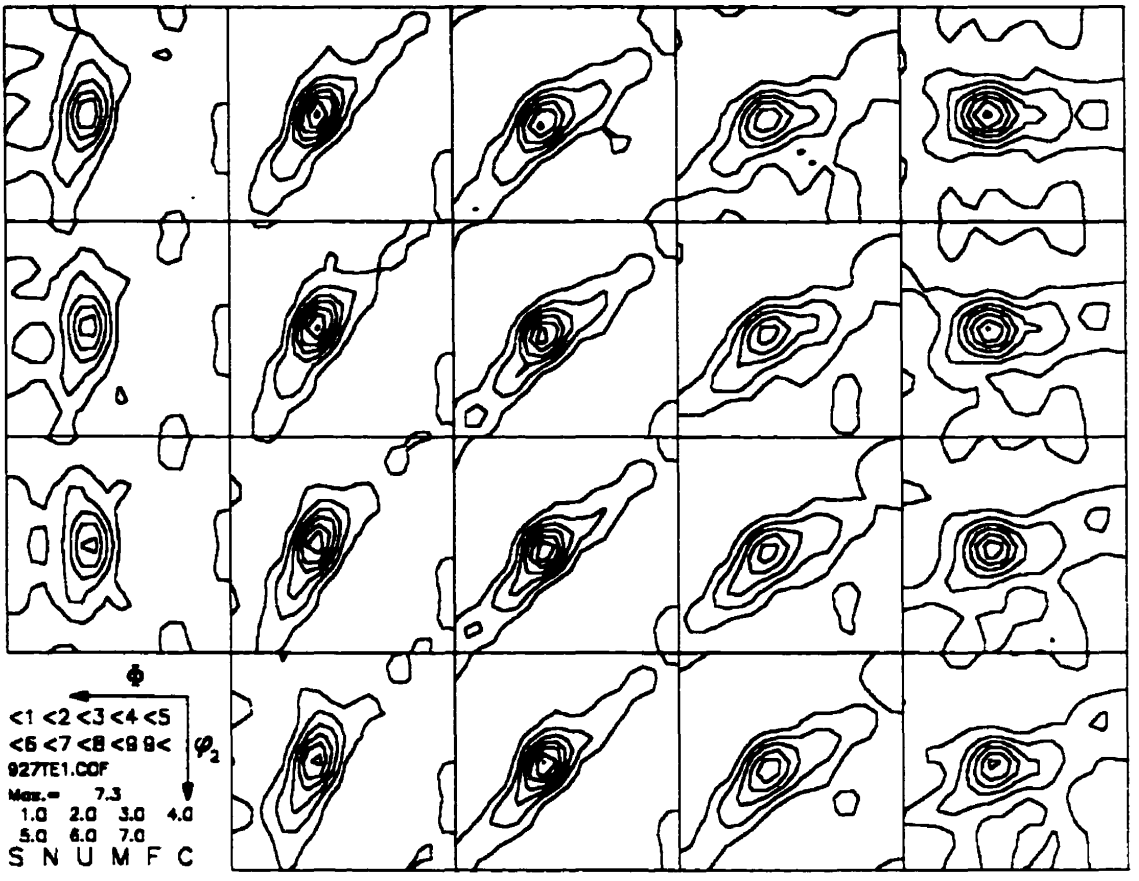

Figure 6. ODF diagram of the enameling steel

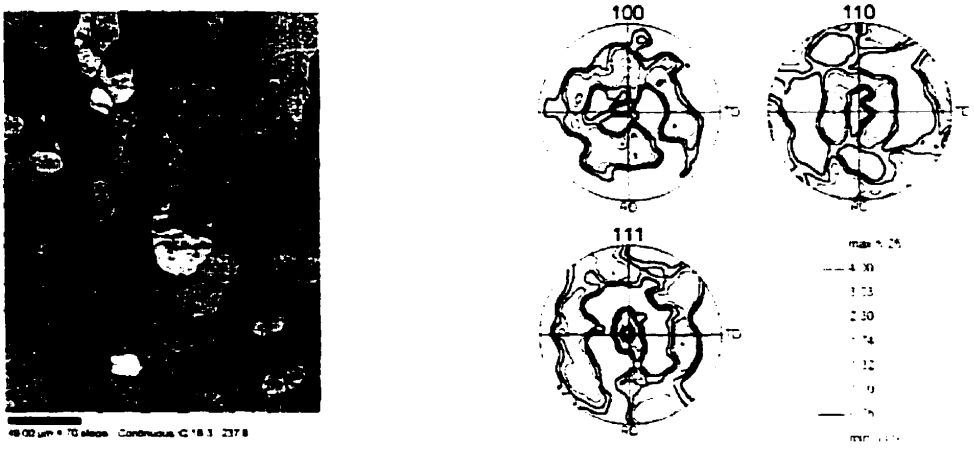

Figure 7. Microstructure and pole figure by OIM

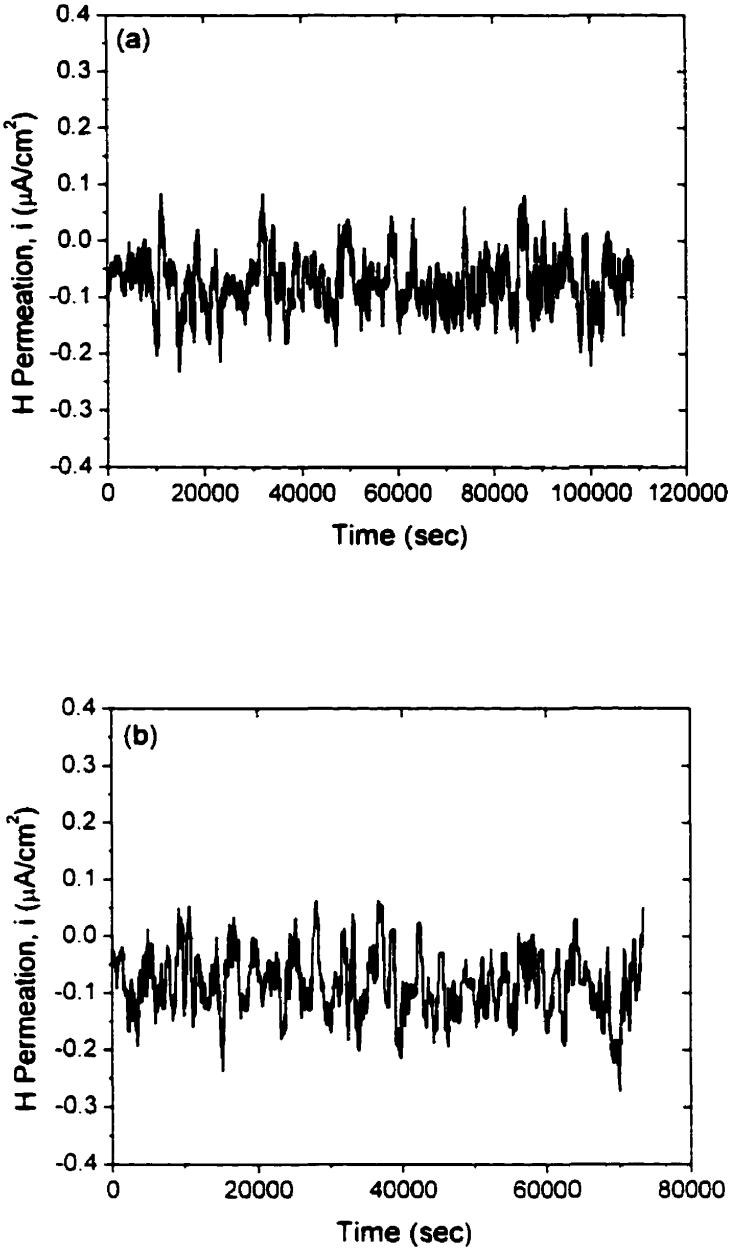

Figure 8. Hydrogen permeation on the enameling steel
(a) thick coating side (b) thin coating side

8 shows that hydrogen is not permeated through the enamel coating layer, irrespective of the thickness of the enamel coating on the steel substrate. This is very reasonable because enamel coatings have no electric conductivity. Therefore, if hydrogen is diffused out from the steel to the enamel coating layer, it cannot penetrate enamel coating but it is rather accumulated on the boundary between the steel substrate and the enamel coating layer. The hydrogen diffused from the steel does not affect the surface cracking of the enamel coating.

4.2.2. Characterizing Defects in Enamel Coating

The defects of enamel coating layer on steel substrate were examined by the Scanning Electron Microscope (SEM) and the result is shown in Photo 2. The sample used in this study was obtained from the enameling steel produced by Dofasco Inc. and all samples were etched by a solution of 3 % Nital. Photo 3 clearly shows the enamel layers coated in both sides of steel substrate. The defects of the coating were found in the upper middle side of enamel coating. Photo 3 is the magnified photo of this cracked section. The voids are shown as small black marks in steel substrate, and the boundary between the enamel coating and the steel substrate is very clear. It is noted that many bubbles are shown in the enamel coated layer. These bubbles were formed during the enamel coating process and they have originated from gas inclusions in the melted enamel bath.[2]

Photo 4 shows the magnified region of a defect free layer. Compared with the defected region shown in Photo 3, no significant difference is found both in the boundary between the steel substrate and the enamel coating and in the enamel coating itself. It is, therefore, very difficult to identify what affects the surface defect formation in enamel coating. In this study, the mechanism of the formation of surface defect is investigated. During polishing, there was a disruption in enamel coating layer caused by the brittle property of the enamel shown in the upper side of Photo 4.

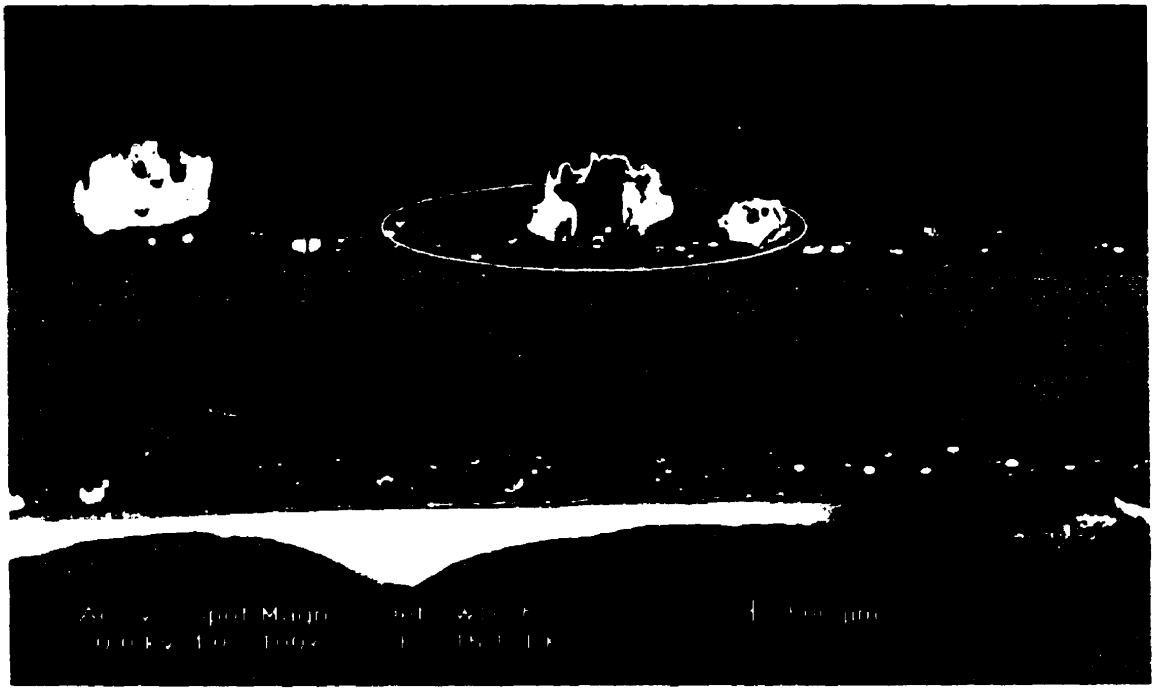

Photo 2. SEM of enamel coating surface defect

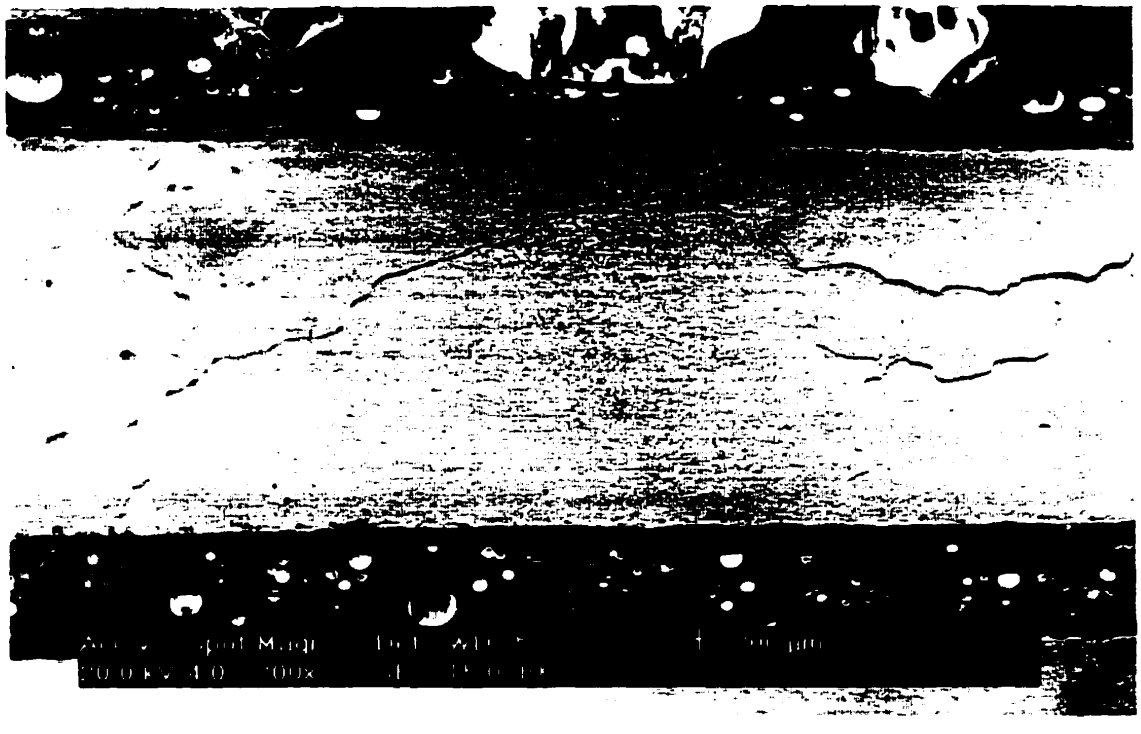

Photo 3. SEM magnification of defect region

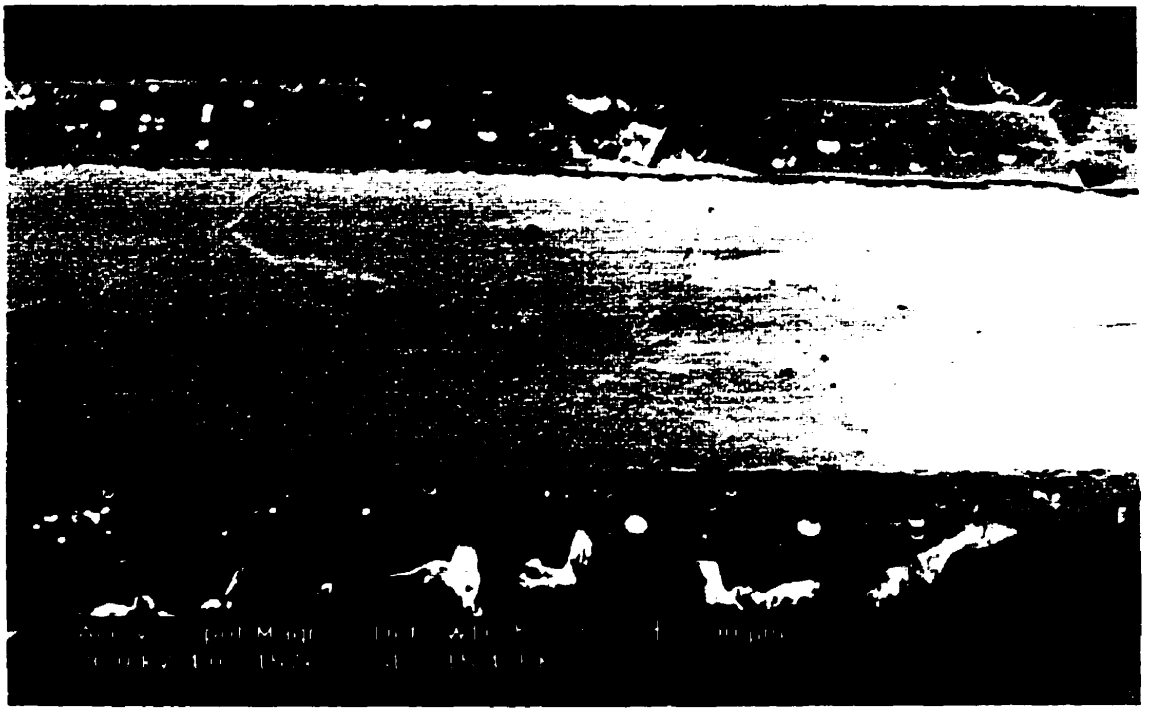

Photo 4. SEM magnification defect-free region

4.3. New Mechanism of Surface Defect Formation in Enamel Coatings

4.3.1. Previous Mechanism of Defects Formation

Many researchers of the industry tried to investigate the mechanism of surface defect formation in enamel coatings.[2,4,40] They claimed the atomic hydrogen diffuses to the enamel-steel interface and forms a large molecular hydrogen. Pressure builds up in these areas and if it attains is high enough values, the enamel layer ruptures and the fish scale defect could form. This is shown schematically in Figure 9. No clear evidence supports this theory of the mechanism of defect formation.

According to this mechanism, there should be some differences in microstructure at the interfaces under the surface defect and the defect-free area because of hydrogen pressure gradients. In particular, one can expect that a high hydrogen pressure might arise if the transport of hydrogen to the surface is facilitated by grain boundaries. Moreover, when comparing Photo 3 (surface defect area) and Photo 4 (defect-free area), one can see that there is no difference in the interfaces between the steel substrate and the enamel coating. Therefore, this mechanism cannot explain the surface defect formation in enamel coating. Nevertheless, one can expect that a high hydrogen pressure might be built if the transport of hydrogen to the surface is facilitated by grain boundaries.

4.3.2. New Mechanism of Defects Formation

To overcome the deficiencies in the theory of the previous mechanism, we suggest the following new mechanism based on obtained experimental results.

a. **Molecular hydrogen pressure**: Since no difference was found in the interface between steel and enamel coating regardless of the defects in enamel surface, it can be reasonably assumed that hydrogen atoms diffused out from steel are accumulated in the interface homogeneously to form molecular hydrogen and exert uniform pressure to the enamel coating.

b. **Gas bubble in enamel coating layer**: The bubbles originated from the gas in the enamel melt are formed in the enamel coating layer. These bubbles can be distributed irregularly. If the bubbles are densely distributed in certain areas, then the cross-sectional area of the enamel coating is reduced. If there is an increase in local density of bubbles in the enamel coating, the stress applied to the coating under the uniform pressure exerted by molecular hydrogen becomes higher. Therefore, this area of enamel can be easily ruptured and surface defects such as fish scale are formed.

The schematic diagram of this new interpretation of formation of defects is shown in Figure 10. Generally speaking, the formation of the surface defect in the enamel coating assumes that there is both a uniform molecular hydrogen pressure on the steel-enamel interface and an irregular distribution of bubbles in the enamel-coating layer. Therefore, in order to prevent the formation of surface defects in the enamel, it is necessary to decrease the hydrogen pressure on the steel-enamel interface, and decrease the possibility of the bubble formation in the enamel coating.

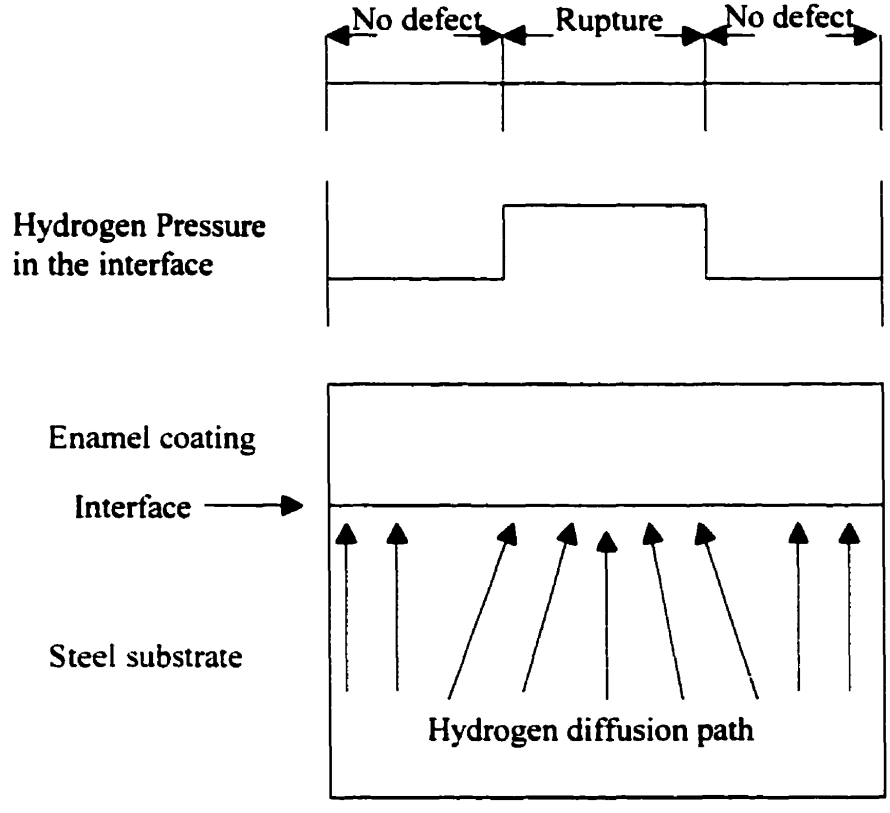

Figure 9. Schematic diagram of the previous mechanism of surface defect formation in enameling steel.

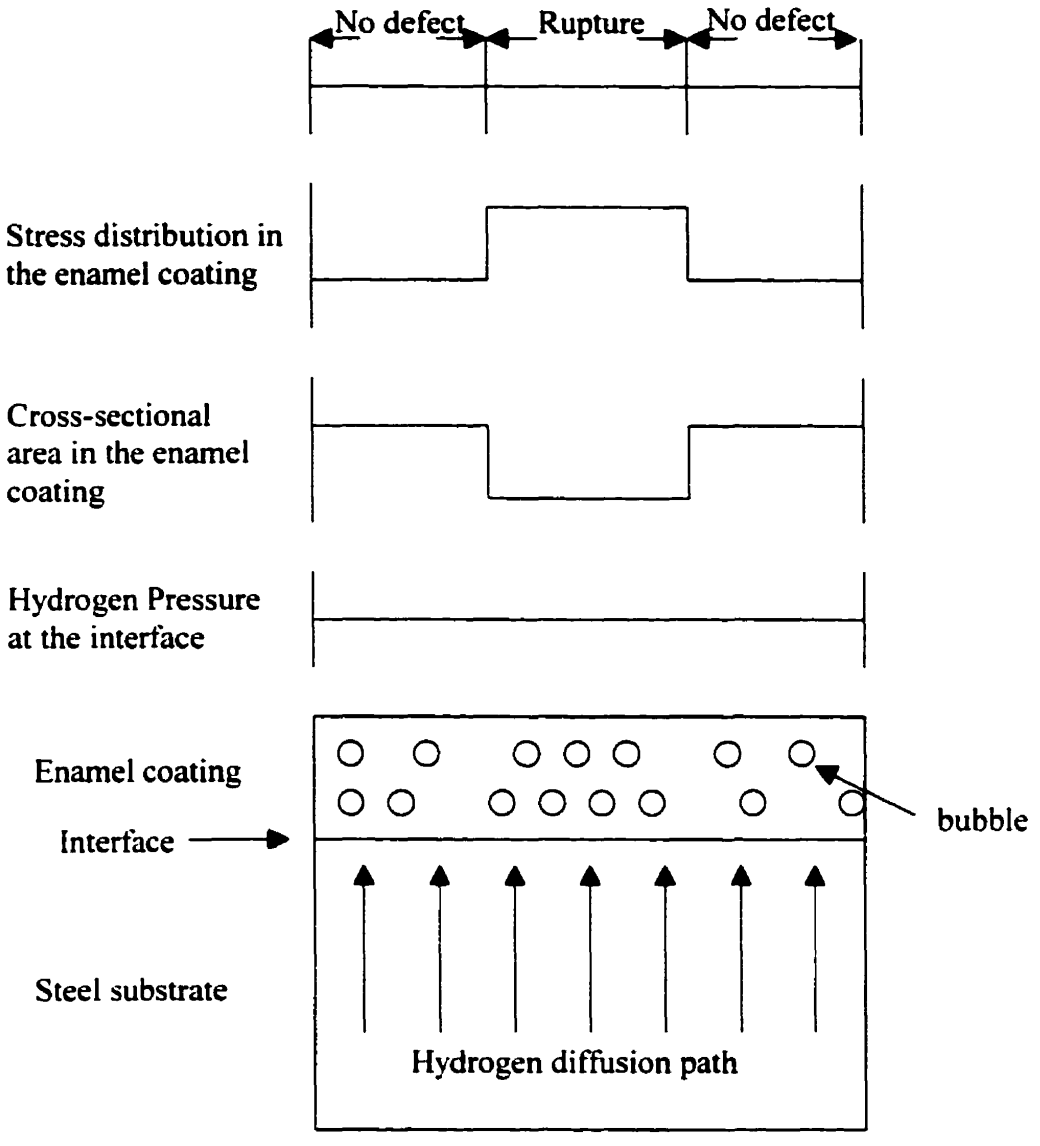

Figure 10. Schematic diagram of the new mechanism of surface defect formation in enameling steel.

4.4. The Factors in Steel Affecting Hydrogen Diffusion

4.4.1. The Effect of Voids on Hydrogen Diffusion

The voids in steel have been known as the hydrogen trap sites and the hydrogen diffusion should lessen as the trap sites number and volume increase. Wu and Norton[4] investigated the relationship between voids area and hydrogen permeability. According to their study, hydrogen permeability had a linear relation with the voids area. They demonstrated that as the voids area increased, the hydrogen emergence time increased as well. From their result, they concluded that if the voids area is larger than a certain critical amount, the hydrogen diffusion could be retarded by voids and fishscale formation could hence be prevented.[4,40]

To describe the distribution of voids in steel substrate, all samples were cut from the steel plate in locations such as edge 1, center, and edge 2 sections shown in Figure 11 and the voids area was investigated. Table 5 shows the distribution of voids area and average grain size of each section of the sample. It shows that the amount of voids area has no trend with the section in slab. It means that the voids formed at cold rolling are randomly distributed in steel slab. The average grain size of the steel is about 15 μm and equiaxed. as illustrated in Figure 7 on page 28 of this paper.

In this study, the relation between the voids area and hydrogen permeation was investigated to learn about the effect of voids area on hydrogen diffusion. Figure 12 shows the variation of voids area with hydrogen permeation emergence (breakthrough time). Here, hydrogen permeability is described as the breakthrough time divided by the square of thickness, like Tb/L^2. Contrary to Wu et al.'s result, no direct relationship between hydrogen permeation and voids area is observed. In other words, there is no significant effect of voids area on hydrogen diffusion. It means that the distributed voids in the steel substrate may act as hydrogen trap sites, but their direct role to the formation of surface defect (fish scale) prevention is questionable.

Figure 13 shows the variation of hydrogen flux with voids area. Hydrogen flux is calculated as follows from the permeation curve data points of Figure 12;

$$\text{Hydrogen Flux} = \int_{t=0}^{t=tf} \frac{i(t)}{A} dt \qquad (4.1)$$

where i is current (μA), A is cross-sectional area (cm^2) and t is time in second. tf was assumed as 10^5 sec.

If hydrogen diffusion is affected by voids area, hydrogen flux should be related to the voids area. According to Figure 13, however, there is no relation between hydrogen flux and voids area. It means that the hydrogen flux is not significantly affected by voids area in investigated steel specimens. This result can be used in support of our conclusion that the hydrogen diffusion has no relation to the voids area in steel.

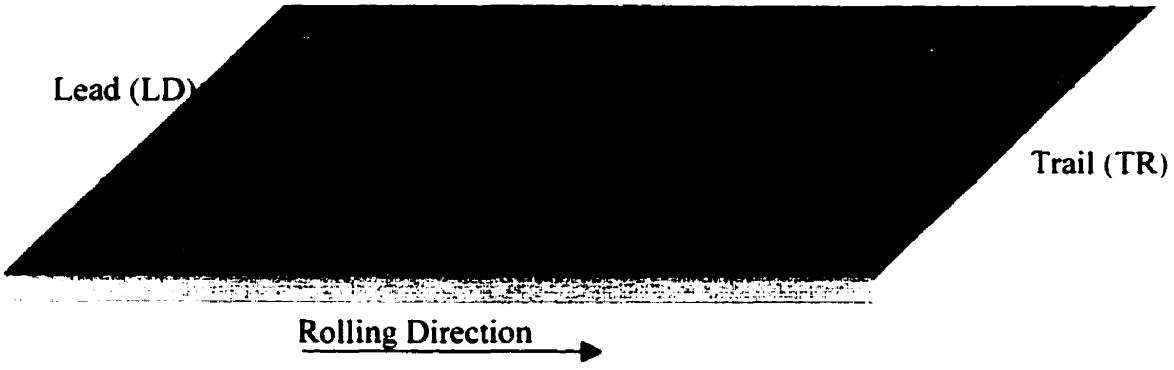

Figure 11. The schematic diagram of sample cutting from the steel plate

Table 5. Voids area of the sample

Sample		88927			88928			88929			88946			KT82108		
		E1	C	E2	E1	C	E2	E1	C	E2	E1	C	E2	E1	C	E2
TR	Void	235	43	61	96	1081	178	36	79	114	100	75	218	238	616	193
	Grain size	15.5	15.4	14.4	18.8	12.9	14.5	13.7	15.7	15.8	14.7	16.7	18.0	18.8	15.0	17.0
LD	Void	100	86	810	248	401	536	146	386	145	151	128	116	399	263	199
	Grain size	14.5	13.3	14.8	13.7	13.2	13.2	18.4	13.5	15.6	19.5	17.6	19.4	17.1	19.4	16.9

Void : total voids area. μm^2: average grain size : μm; TR : trail part and LD : lead part

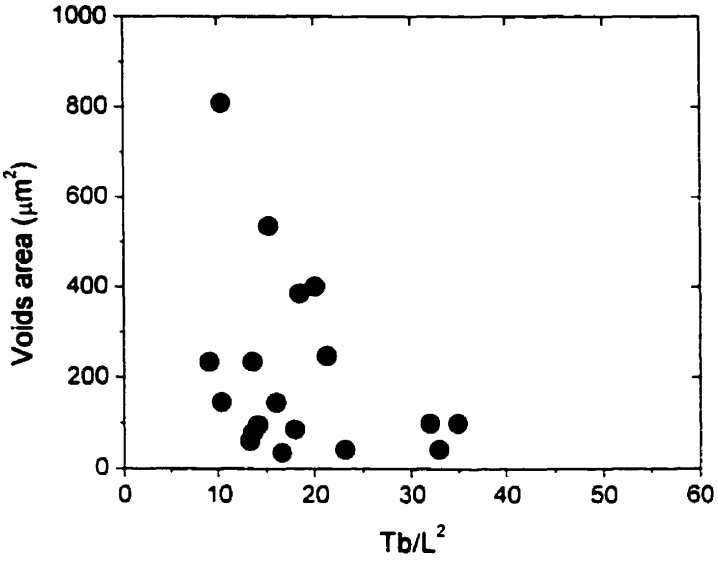

Figure 12. Voids area vs. breakthrough time

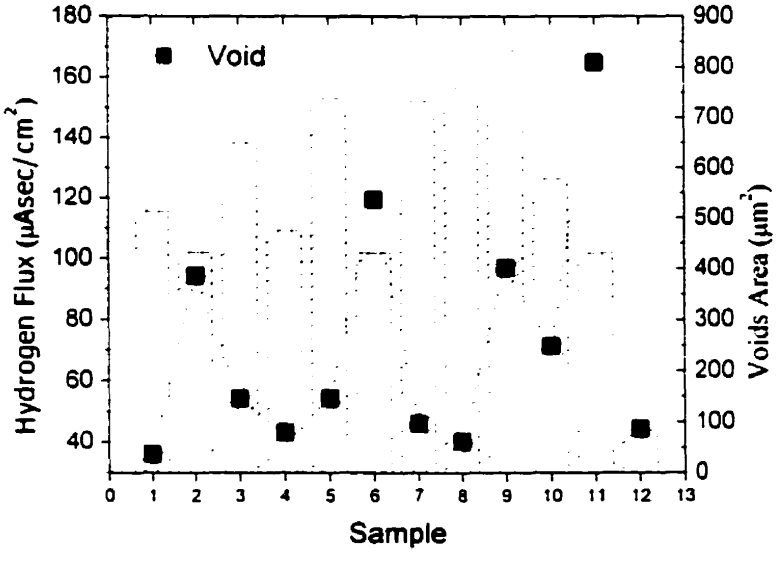

Figure 13. Hydrogen flux vs. voids area

1) 88929TRE1 2) 88929LDC 3) 88929LDE2 4) 88929TRC

5) 88929LDE 6) 88928LDE2 7) 88928TRE1 8)88927TRE2

9) 88928LDC 10) 88928LDE1 11) 88927LDE2 12) 88927LDC

4.4.2. The Effect of Cold Rolling on Hydrogen Diffusion

To discover the effects of cold rolling on hydrogen diffusion, four specimens have been cold rolled to different reductions. These specimens were examined using hydrogen permeation test equipment.

1) Microstructure After Cold Rolling

Photo 5 shows the variation of the microstructure of each specimen with cold rolling. The densities of dislocation and micro-voids increase significantly as shape is elongated and the cold rolling is reduction increased; the grain reveals the typical rolling characteristics of the pan-cake type microstructure, observed in Photo 5. The major difference between cold rolling specimens is in the density of dislocations, the amount of micro-voids, and by the shape of the grains.

2) Characteristics of Hydrogen Permeation Curves after Cold Rolling: Transition Phenomenon from Non-Equilibrium State to Steady State.

Figure 14 shows the effect of cold rolling on the variation of hydrogen permeation through steel. Curve 1 is the hydrogen permeation for steel before cold rolling and curve 2, 3, 4 and 5 are those for cold rolled steels with reductions of 50, 70, 80 and 90%, respectively.

All specimens attain steady state after 50,000 seconds, although curve 1 might have fluctuated from experimental errors. However, there are clear transient peaks observed in the hydrogen permeation curves in the case of cold rolled steels, which are not seen in the steel that was not cold rolled. Moreover, the height of peak, which is defined as the difference between the maximum permeation flux and steady state one, increases with increasing cold rolling rate. This kind of phenomenon is not yet well understood.

Only Manolatos et al. tried to explain this kind of peak by the formation of a passive layer.[25-27] They claimed that the passive film could be formed on the exit side of the steel substrate during hydrogen permeation experiment and this film could block the diffusion

a) original

b) 50% reduction

c) 70% reduction

d) 80% reduction

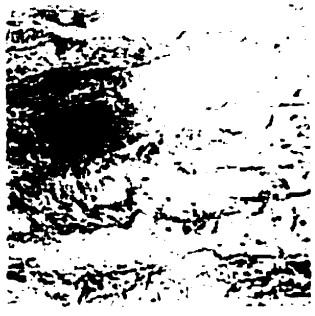

e) 90% reduction

Photo 5. Optical microstructure (1000X) of cold rolled sample

of hydrogen, which results in the increase of concentration of hydrogen to values above zero. If the concentration of hydrogen at the exit side is higher than zero, it means that it is impossible to reach steady state. Therefore, they concluded that hydrogen permeation cannot arrive at steady state and it decrease after peak when the passive layer formed at the exit side. But their assumption cannot explain the present results that show that there is a peak followed by steady state for cold rolled steel and there is no peak in specimens that are not rolled (curve 1).

In order to explain the present result, a novel explanation is offered in this work. A transition phenomenon from the non-equilibrium state to the steady state is proposed. Figure 15 shows a schematic diagram illustrating this new explanation. The reason for the peak to occur in the cold rolled steel is that the hydrogen permeation increases at a higher rate than in the equilibrium steady state. One can therefore a "non-equilibirum supersaturated state" because there is high residual energy in cold rolled steel. After reaching a certain level of supersaturated state, it goes to equilibrium steady state which has a constant permeability.

If the residual energy in steel decreases, then the ratio of supersaturation lessens and the height of peak thus becomes lower and lower. The peak does not appear in no cold rolled steel means low residual energy. This new proposed transition phenomenon from non-equilibrium state to steady state can easily explain all behaviors of experimental results in the present study. It may be said that in the study of Manolatos et al., the experimental duration time was not enough for hydrogen permeation to reach steady state.

3) The Effect of Cold Rolling (Dislocation) on Hydrogen Diffusion.

On the basis of the result shown in Figure 14, the diffusion coefficients of hydrogen in cold rolled steels were calculated by the time lag method. It is noted that the steady state is considered as a standard for this calculation by considering the result explained in the previous section.

Figure 16 shows the variation of hydrogen diffusion coefficient with the rate of cold rolling. The diffusion coefficient of hydrogen decreases steeply with the increase of cold rolling. It even becomes one tenth of non cold rolled specimen after 90% cold rolling. It is necessary to determine what microstructural parameters are responsible for the change of hydrogen diffusion coefficient in cold rolled steel. As pointed out in the previous section, the amount of dislocation, micro-voids, and grain size increases as the rate of cold rolling augments. It was already concluded that the amount of voids does not influence the diffusion. Therefore, the decrease of hydrogen diffusion coefficient results from the increase of the density of dislocation. This is in good agreement with previous investigation.[7]

The height of hydrogen permeability at steady state also increases with increasing density of dislocations. These are related to the hydrogen flux. Figure 17 shows the variation of hydrogen flux with the density of dislocations. It can be calculated by the following equation, in consideration of Figure 2.

$$Hydrogen\ flux(J) = D\frac{C_0 - C_L}{L} = \frac{i_\infty}{F} \qquad (4.2)$$

Figure 17 shows that the hydrogen flux increased as the density of dislocation increased, while hydrogen diffusion coefficient decreased. As shown in Equation (4.2), the hydrogen flux depends on the hydrogen concentration in steel as well as the hydrogen diffusion coefficient. If the density of dislocation is increased, the hydrogen concentration is increased because the dislocations play roles in hydrogen trap sites, as previously discussed. Therefore, the hydrogen flux can be increased with cold rolling because the amount of increased hydrogen concentration is larger than that of decreased hydrogen diffusion coefficient by the dislocations.

Figure 14 also shows the decay pattern of hydrogen permeation for each specimen after the current of the cathode side was turned off. The decay rate is related to the dislocation density of the steel substrate. This result ascertains the proposal of Beachem who claimed that the effect of hydrogen is to enhance dislocation motion.[17] Finally, it is

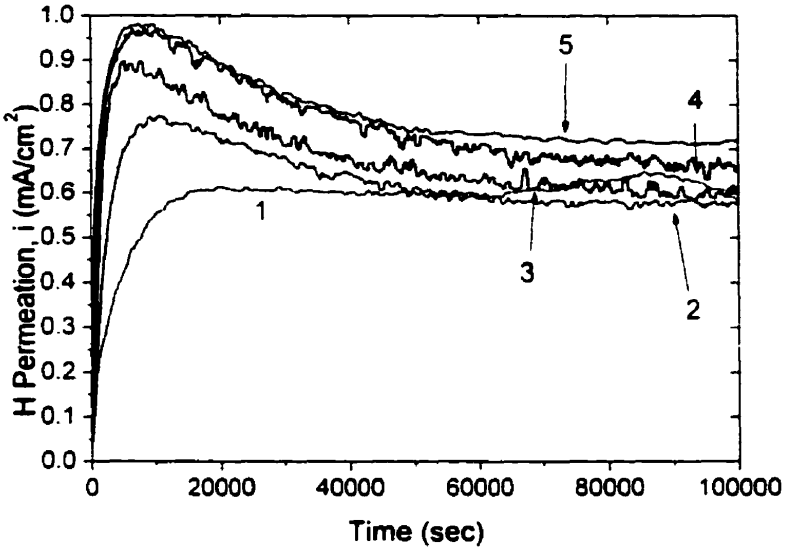

a) hydrogen permeation curves

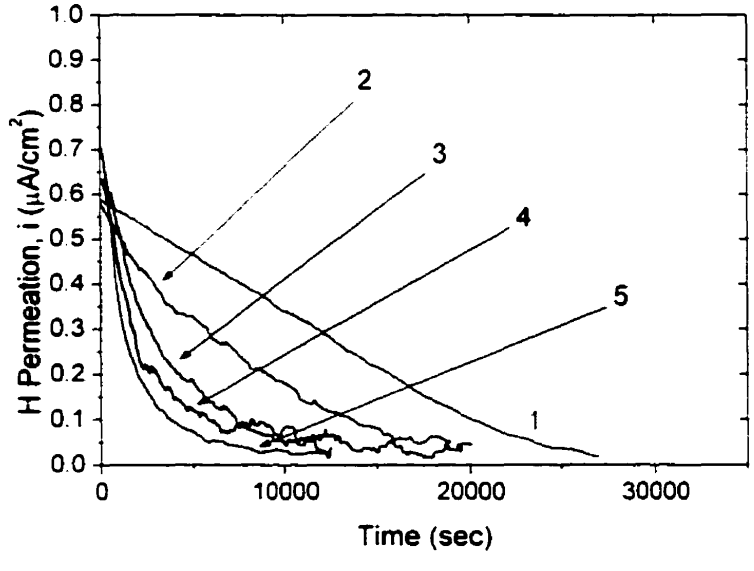

b) decay curves

Figure 14. The effect of cold rolling reduction on permeation curve
1) 0% 2) 50% 3) 70% 4) 80% 5) 90% cold rolled

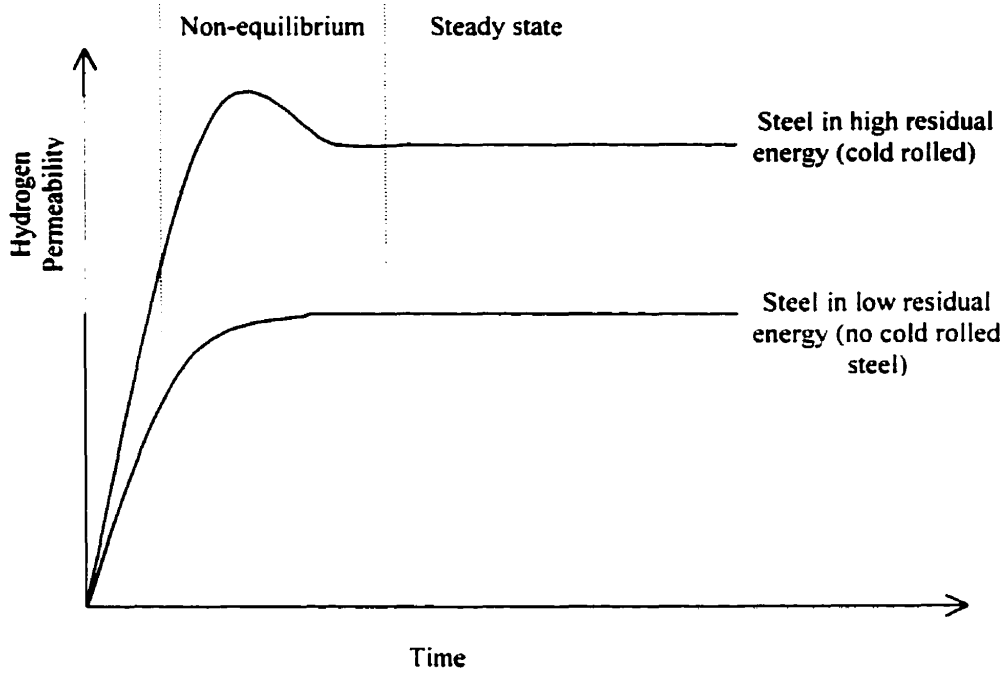

Figure 15. Model of transition of hydrogen permeability from the non-equilibrium to steady state

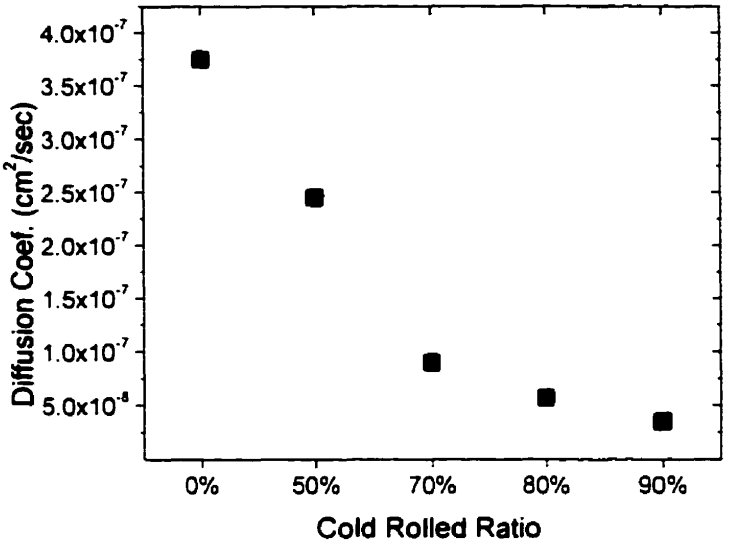

Figure 16. Hydrogen diffusion coefficient of cold rolled samples

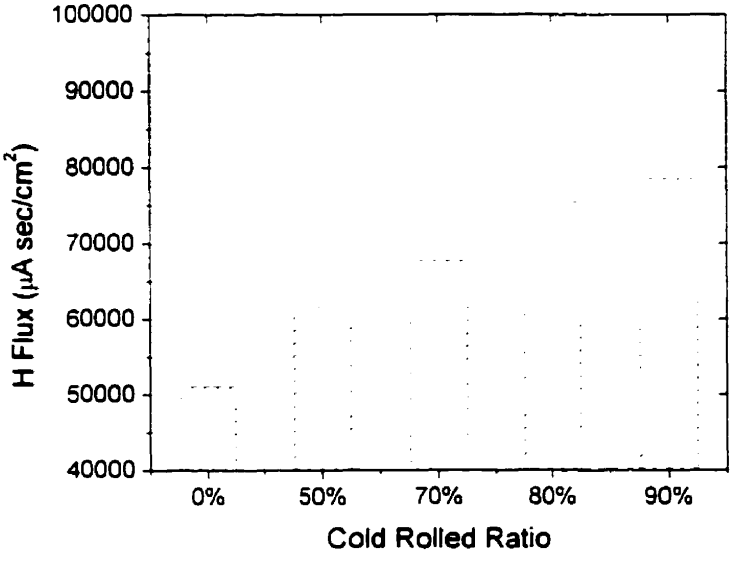

Figure 17. Hydrogen flux of cold rolled samples

concluded that the high dislocation density increases the diffusion flux of hydrogen in steel.

4.4.3. The Effect of Surface Roughness

Surface conditions could affect the hydrogen diffusion. Y. P. Zheng and T. Y. Zhang showed that the activation energy for the absorption at the surface of the sample is affected by the surface cleaning conditions.[16] Bellati and Lussana observed that polished iron specimens were more rapidly penetrated by hydrogen than rough surfaces.[8] However, no investigations have been done to establish the effect of surface roughness on hydrogen diffusion.

To evaluate the effect of surface roughness, three kinds of specimens with different surface roughness were prepared. Then, the hydrogen permeation tests were carried out under the same conditions. Figure 18 shows the effect of surface roughness on the hydrogen diffusion in steel. Curves 1, 2 and 3 are hydrogen permeation curves for the steels polished on both sides using sequentially 0.05 μm colloidal silica solution, 600 grit (particle size of 14 μm) and #120 (particle size of 125 μm) emery paper. To prevent the cold working during polishing, the specimens were carefully handled at lowest speeds possible.

The diffusion coefficient calculated from the time lag method is shown in Figure 19. Notwithstanding experimental error, the diffusion coefficient seems to be independent of the surface roughness of the steel substrate. It means that the diffusion coefficient is determined not by the surface roughness but rather by the internal microstructure of the steel substrate. The decay rate of hydrogen permeability shown in Figure 18 also indicates that the diffusion coefficient related to the slope is independent of surface roughness.

The hydrogen flux calculated from Equation (1) shows its maximum at a surface roughness of 600 grit emery paper. Both the finer and rougher surface roughness decrease hydrogen flux. It means that there is a maximum hydrogen diffusion coefficient

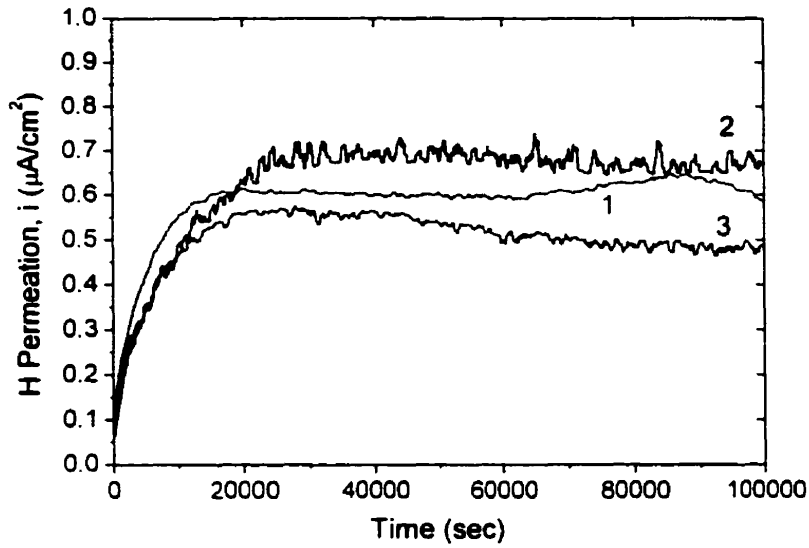

a) hydrogen permeation curves

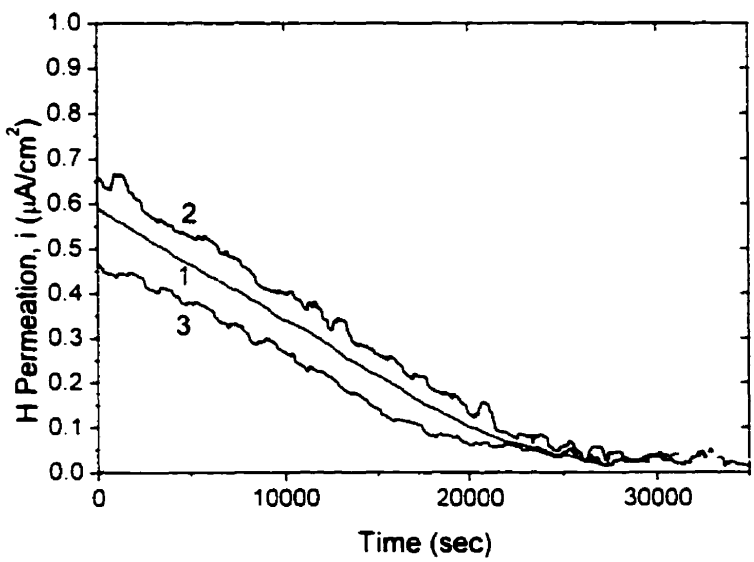

b) decay curves

Figure 18. Surface roughness effect on hydrogen permeation

1) fine polished with 0.05 μm colloidal silica solution

2) polished with 14 μm particle size (600 grit) emery paper

3) polished with 125 μm particle size (120#) emery paper

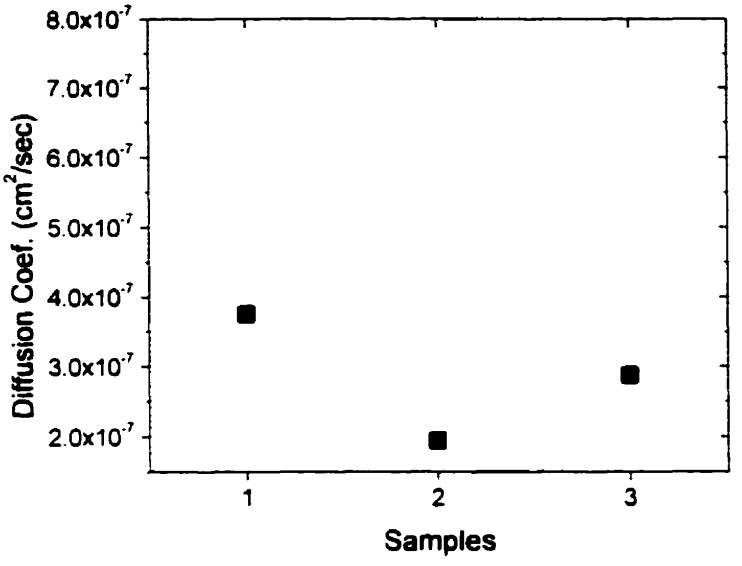

Figure 19. Hydrogen diffusion coefficient variation of different surface roughness

1) fine polished with 0.05 μm colloidal silica solution

2) polished with 14 μm particle size (600 grit) emery paper

3) polished with 125 μm particle size (120#) emery paper

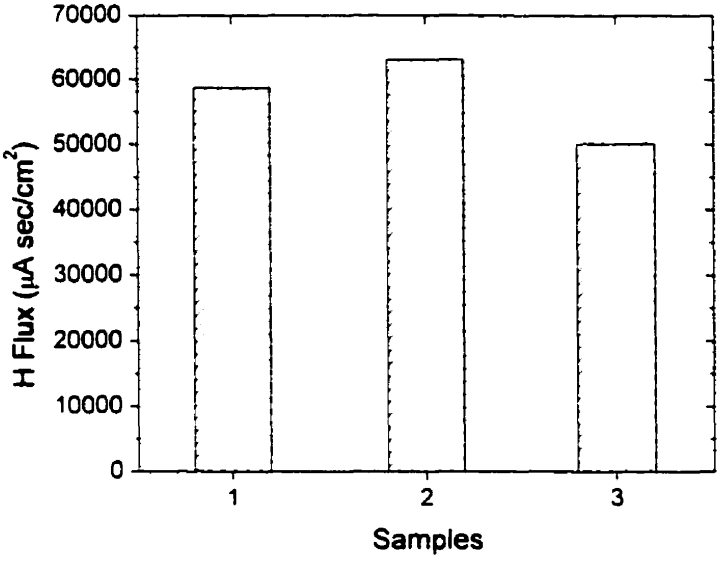

Figure 20. Hydrogen flux variation of different surface roughness samples

1) fine polished with 0.05 μm colloidal silica solution

2) polished with 14 μm particle size (600 grit) emery paper

3) polished with 125 μm particle size (120#) emery paper

for a certain surface roughness. When the surface roughness becomes finer, the free surface area increases. The larger free surface area corresponds to a higher surface energy. If the surface energy becomes high on the exit surface of a steel substrate, it becomes more difficult to desorb the hydrogen from the exit side. This plays a role in the hindrance of hydrogen diffusion from steel as it feeds back to increase the concentration of hydrogen at the entry side.[25-27] On the contrary, if the surface is too fine like that of glasses, the free surface area becomes to be minimal. Then, the hydrogen concentration at the entry side is reduced by low surface energy. Finally, the hydrogen flux has a maximum value at certain surface roughness.

4.4.4. The Effect of Passive Film on Hydrogen Diffusion

The iron or steel surface is apt to react with the surrounding atmosphere, producing oxide films such as FeO or Fe_3O_4 on the surface. A passive film can be easily formed on the surface if either one is immersed in an electrolytic solution. The effect of passive film on the diffusion of hydrogen might be complicated.

It is rather difficult to observe the passive film on the surface of steel directly. Therefore, a consecutive permeation technique was adopted in this work. Pressouyer and his co-workers established the consecutive permeation technique in order to evaluate the hydrogen trapping effects. [10-13] This technique is commonly used to find the effect of passive layer on hydrogen diffusion.

Figure 21 and 22 show the consecutive tests for the specimen having a fine surface (0.05 μm) and a rough surface (14 μm), respectively. Curve 1 was obtained from the first permeation test consecutively followed by the second experiment shown in Curve 2. There was a decay procedure between the first and second permeation experiment for the passive film to be formed on the surface of the steel specimen. After the second experiment (Curve 2), the specimen was polished again, and the passive film was removed. Afterwards, the hydrogen permeation test was performed again and Curve 3 was obtained. The consecutive experiments in Figures 21 and 22 show that passive films

reduce both the diffusion coefficient and the flux of hydrogen by about 50 %. Moreover, Curve 3 is almost the same as Curve 1.

According to Pressouyer et al., hydrogen trap sites could be filled during the first transient rise, so the second transient rise should be faster than the first one which should slow down by irreversible trapping.[12] Comparing the Curve 1 and 2, the second transient rise curve is slower than the first one. This is completely contradictory to explanations offered by Pressouyer et al. The third experiment (Curve 3) was performed to explain this contradiction. Curves 1 and 3 are almost identical. It means that there is no irreversible factor to trap hydrogen in steel.

In addition, the amount of the reduced hydrogen flux by the passive layer is almost the same as that of the hydrogen diffusion coefficient. Considering Equation (1), this means that the reduction of the hydrogen flux results from a decreased hydrogen diffusion coefficient. In other words, the passive layer formed on a steel surface does not influence the hydrogen concentration at the entry side.

Iron or iron based alloys in near neutral solutions are normally covered with films containing $Fe(OH)_2$, Fe_3O4, or FeOOH of thickness of 20~30 Å.[33,41-44] Either H^+ as H_3O^+ or OH^- may fill a more direct role in passive film formation. Electrochemical measurements on steel in anhydrous to an aqueous electrolyte, showed no evidence of active-passive behavior although an oxidation-reduction half-cell electrode potential could be measured readily for oxygen. Active-passive behavior is absent in other non-aqueous electrolytes as well. The overall anodic reaction

$$Fe + 2H_2O \rightarrow Fe(OH)_2 + 2H^+ + 2e^-$$

is approximate and assumes a certain phase, $Fe(OH)_2$, which may or may not be attained eventually in the film structure.[19] From the results of consecutive permeation experiments, the existence of a passive layer can be used to explain the observation but it is rather difficult to identify it. X-ray diffraction methods were used to identify the passive layer but this trial was not successful.

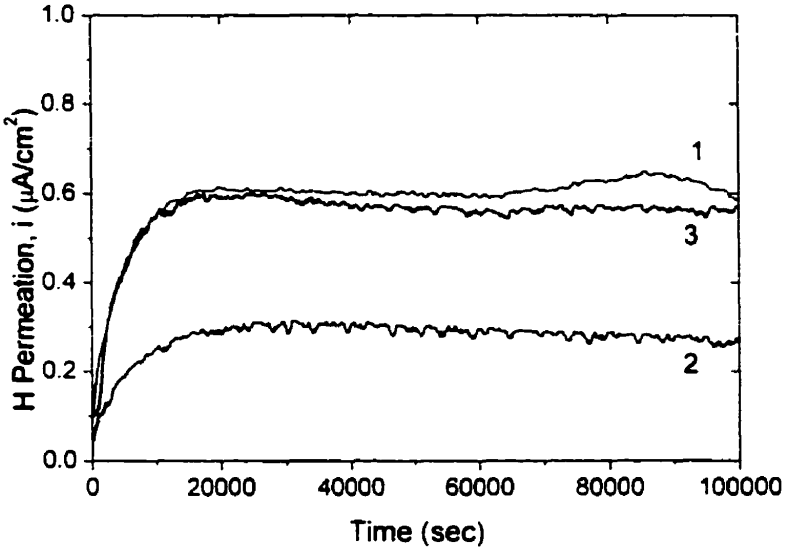

Figure 21. Consecutive test on fine polished sample

1) 1st transient rise 2) 2nd transient rise 3) transient rise after repolishing of the sample

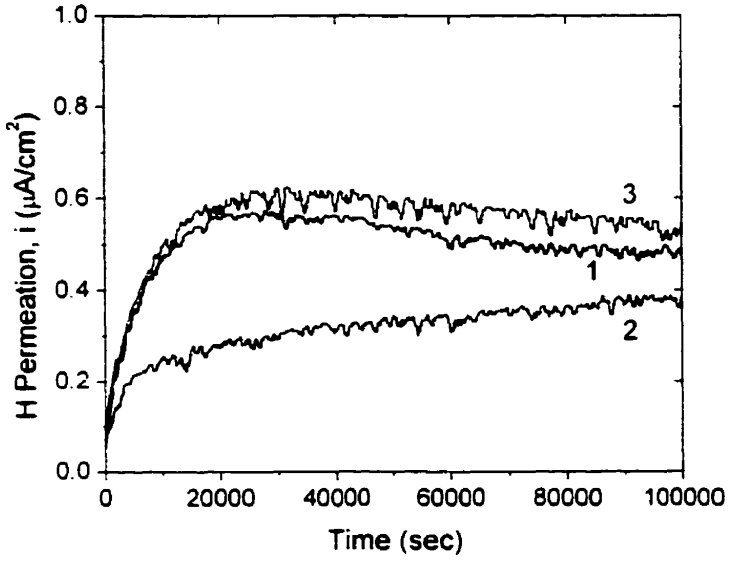

Figure 22. Consecutive test on 120# emery polished sample

1) 1st transient rise 2) 2nd transient rise 3) transient rise after repolishing of the sample

4.4.5. The Effect of Palladium Coating on Permeation Results

Iron or steel tends to corrode in aqueous solution over the whole pH range.[45] A noble metal coating such as palladium has been commonly applied to the steel surface of the exit side to prevent the dissolution and formation of passive film on the anode side.

To assess the effect of the palladium coating on the hydrogen diffusion, the coating was applied to the exit side of samples by plasma sputtering methods. First of all, samples were polished using different grades of paper so that they have a different surface roughness. Then, plasma sputtering experiments were carried for times between 3 and 8 minutes to obtain the optimum palladium coating thickness. The coated samples were investigated using the apparatus for hydrogen permeation measurement.

1) The Effect of Palladium Coating

Figure 23 shows the variation of hydrogen permeability with roughness of steel substrate coated by a 200 Å Pd layer. Curves 1, 2 and 3 are obtained from steel substrates whose surface roughnesses are qualified as fine, intermediate and rough, respectively. Although Curve 3 deviates a little from the other curves, hydrogen diffusion coefficient and flux are almost the same. It means that Pd coating on the exit makes hydrogen permeabilities equivalent, regardless of the roughness of the steel surface. Differences in the surface roughness at the entry side influence the hydrogen diffusion if a Pd coating is present at the exit side. This experiment proves that the diffusion in steel is determined not by the surface layer at the entry side but by the one at the exit side.

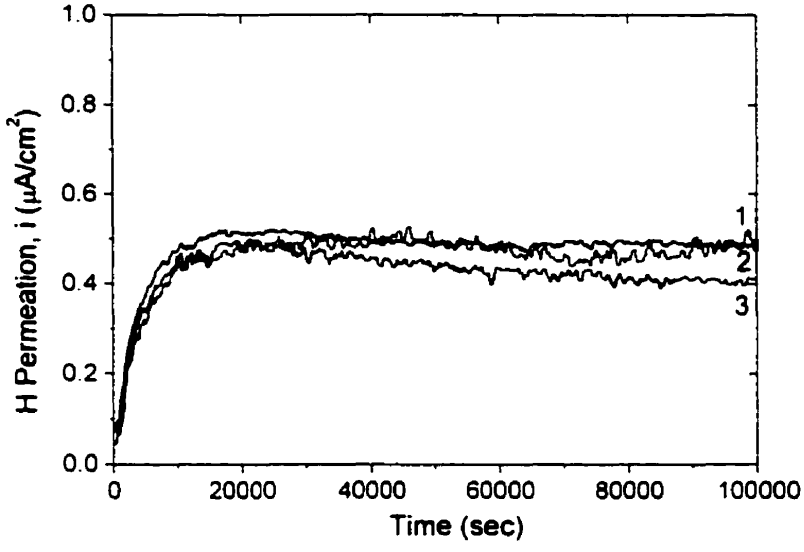

Figure 23. Hydrogen permeation curves after 200 Å Pd coating

1) fine polished with 0.05 μm colloidal silica solution

2) polished with 14 μm particle size (600 grit) emery paper

3) polished with 125 μm particle size (120#) emery paper

2) The Effect of Palladium Coating on the Hydrogen Diffusion

To find the effect of Pd coating on the hydrogen diffusion, hydrogen permeability for Pd coated steel was compared with that for without coated steel. These results are shown in Figure 24. Curves 1 and 2 were obtained from no coated steel substrate and from Pd 200 Å coated steel, respectively. After Pd coating, the hydrogen diffusion coefficient was not affected, while the hydrogen flux was reduced by about 15 %. Hydrogen flux is shown in Figure 27. Therefore, it can be concluded that the hydrogen concentration is reduced by the Pd coating since the surface energy of a steel substrate is reduced by the Pd coating. Finally, the reason for the reduction of hydrogen flux by Pd coating is different from that by passive layer explained in the previous section.

3) The Effect of β-Palladium Hydride on Hydrogen Diffusion[22]

To determine the probability of formation of β-Pd hydride and the effect of β-Pd hydride on hydrogen permeability, the following experiment was conducted. Palladium is known as a very noble metal; it therefore does not produce any passive layer. However, if Palladium is under high hydrogen concentration, it can turn into a β-Pd hydride. Once a β-Pd hydride is formed, it hinders hydrogen permeation.

Curve 3 in Figure 24 is obtained in the consecutive second experiment for the same steel coated by Pd 200 Å. Because of high hydrogen concentration produced by high cathodic potentials of 1 mA/cm^2, the coated Pd could turn into a β-Pd hydride. Devanathan and Stachurski reported that when the cathodic potentials was about 10^{-5} A/cm^2, palladium did not transform to β-Pd because the diffusion of hydrogen was only 10^{-10} g atomH_2/sec, a value negligible when compared to the solubility in palladium. On the other hand, the cathodic potentials used in this study were higher than that used by Devanathan and Stachurski by several orders of magnitude, potentially aiding in the fprmation of β-Pd hydride. Curve 3 in Figure 24 is lower than Curve 2 and it indicates that palladium was transformed into unstable β-Pd hydride. It could be concluded that the diffusion coefficient and the flux of hydrogen were reduced by the formation of β-Pd hydride.

Curve 4 was obtained from the specimen after additional coating by a 300 Å Pd layer on the same steel substrate used in the consecutive experiment. This additional palladium layer does not have any major effect on hydrogen permeability. It means that once β-Pd hydride is formed, it is the rate-controlling step for hydrogen diffusion. Therefore, great caution is required to ensure that the Pd coating that used for hydrogen diffusion control does not form β-Pd hydride.

Figure 25 and 26 show the same result that Pd coating has on hydrogen diffusion, much like Figure 24.

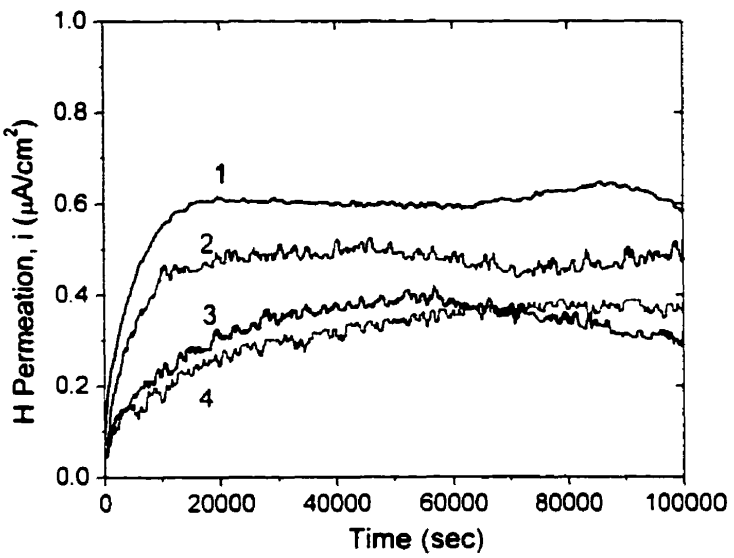

Figure 24. Hydrogen permeation curves of fine polished sample

1) fine polished with 0.05 μm colloidal silica solution

2) 200 Å palladium coating deposited on the exit side

3) 2nd rise on the 200 Å palladium coating deposited on the exit side

4) 500 Å palladium coating deposited on the exit side

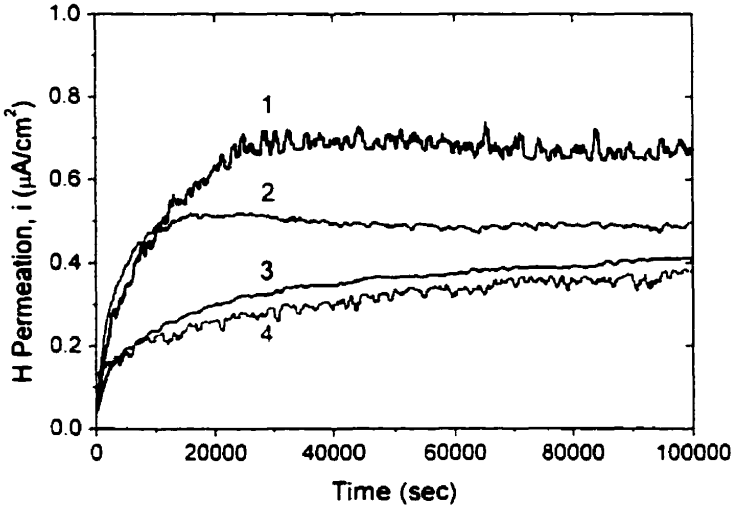

Figure 25. Hydrogen permeation curves of sample polished by 600 grit emery paper

1) polished with 14 μm particle size emery paper

2) 200 Å palladium coating deposited on the exit side

3) 2nd rise on the 200 Å palladium coating deposited on the exit side

4) 500 Å palladium coating deposited on the exit side

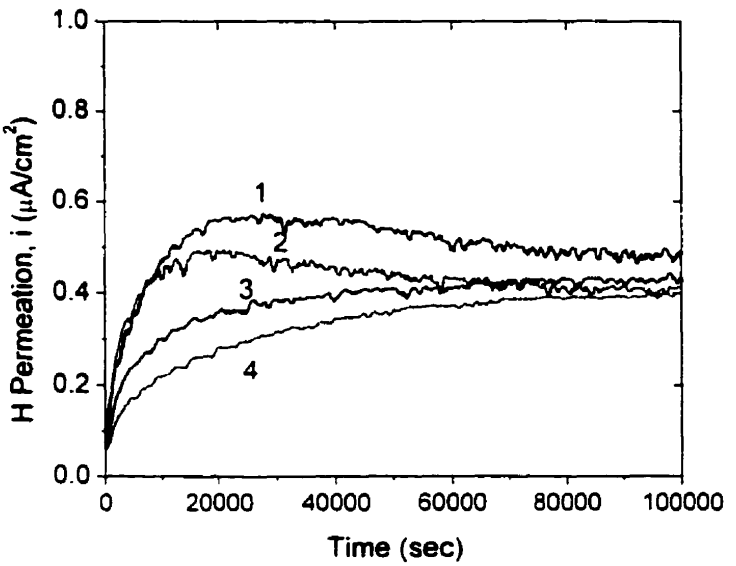

Figure 26. Hydrogen permeation curves of sample polished by 120# emery paper

1) polished with 125 μm particle size emery paper

2) 200 Å palladium coating deposited on the exit side

3) 2nd rise on the 200 Å palladium coating deposited on the exit side

4) 500 Å palladium coating deposited on the exit side

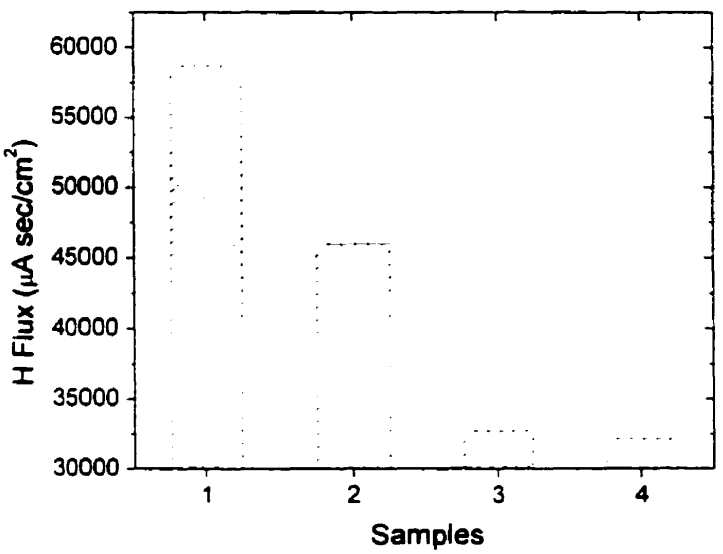

Figure 27. Hydrogen flux variation of fine polished sample

1) fine polished with 0.05 μm colloidal silica solution

2) 200 Å palladium coating deposited on the exit side

3) 2nd rise on the 200 Å palladium coating deposited on the exit side

4) 500 Å palladium coating deposited on the exit side

CHAPTER V.

Suggestions and Comments

This study detailed the way in which steel and enamel coating parameters affect hydrogen diffusion. The several factors are summarized and listed in Table 4. The effect of each factor on hydrogen diffusion was considered under three aspects: the effects on the hydrogen diffusion coefficient, the hydrogen concentration, and the hydrogen flux. It has been studied that considerable amount of hydrogen was dissolved in steel during the procedure of enamel coating. A new mechanism of surface defect formation in enameling steel was also proposed. Based on the factors and the proposed enamel coating rupture mechanism, we can reach the following practical conclusion for industry. In order to reduce defects (fish scale) on the enamel coating surface, the following factors should be considered.

A. The steel substrate should contain less hydrogen and the diffusion of hydrogen to the steel/enamel interface should be diminished.

1) Porosity does not have strong influence on the hydrogen diffusion.

2) Density of dislocation (cold rolling): A high dislocation density can increase the hydrogen flux although it reduces the hydrogen diffusion coefficient. Hydrogen flux is directly related to the amount of hydrogen and, consequently to the surface defects. Considering the hydrogen flux, therefore, it is recommended to reduce high stored deformation energy of steel by optimizing the heat treatment before the enameling process.

3) Surface roughness: Even though it does not significantly influence the hydrogen diffusion coefficient, it could maximize the hydrogen flux at a given surface roughness of steel substrate. Therefore, great care is essential to avoid this certain range of surface roughness when treating the steel surfaces. Surface roughness effect should be investigated in more detail to pinpoint the exact range of surface roughness at which the hydrogen diffusion flux becomes maximal.

B. Oxidation of the surface of steel substrate before enamel coating is deposited.

1) Passive layer: It considerably reduces the hydrogen diffusion. However, a more careful consideration is needed. Because the passive film can significantly retard the diffusion through the passive layer, the hydrogen becomes accumulated on the steel-passive layer interface instead of the steel-enamel coating. It is very difficult to be sure whether this passive layer can endure the homogeneous hydrogen pressure under this layer or not. If it has enough strength to sustain the hydrogen pressure, then it can be very effective in reducing the possibility of surface defects of the enamel coating. Further investigation is necessary.

2) Pd coating: It is very expensive to coat Pd on the steel substrate although it can reduce the hydrogen diffusion. Therefore, it is of no interest in industry.

C. Gas bubbling in enamel coating should be controlled.

Many bubbles are always formed during an enamel coating process. They are randomly distributed on the inside of the enamel coating. As pointed out while discussing the mechanism of surface defect formation, the dense population of bubbles is responsible for the stress at certain regions, this resulting in regional ruptures when the hydrogen gas is under pressure. Therefore, a careful treatment is necessary to prevent local concentrations of bubble.

Table 6. Summary of factors affecting hydrogen diffusion in investigated steel

Factors		Hydrogen Diffusion Coefficient	Hydrogen Concentration	Hydrogen Flux
Steel Substrate	Void	-	-	No effect
	Dislocation (Cold Rolling)	Decreased	Increased significantly	Increased
	Surface Roughness	No effect	Maximum at certain roughness	Maximum at certain roughness
Coating on Steel Surface	Passive Layer (Hydroxide, oxide)	Reduced by 50%	No effect	Reduced by 50%
	Pd Coating	No effect (Remove surface roughness effect)	Decreased	Decreased by 15% (Remove surface roughness effect)
	β-Pd Hydride	Reduced by 50%	Small or no effect	Reduced by 30%
	Enamel Coating	-	-	No effect

CHAPTER VI.

Conclusions

In this study, general aspects of hydrogen diffusion in enameling steel have been investigated to prevent the formation of surface defects on enamel coatings in steel. First of all, a careful observation of a cracked surface of the enameling steel was completed. Then, the effects of several factors on hydrogen diffusion in low carbon steel were investigated by using hydrogen permeation experiment. The following facts summarize the results.

1) A new mechanism of surface defect formation in enameling steel was suggested based on the observation of the microstructure of cracked surfaces of enameling steels. According to this mechanism, the formation of surface defect in the enamel coating is caused by the irregular distribution of bubbles in enamel coating layer under uniform molecular hydrogen pressure on the steel/enamel interface.

2) After considering the results of many hydrogen permeation experiments, transition phenomenon from non-equilibrium to steady state in hydrogen permeability was newly proposed to explain the shape of hydrogen permeation curves. That is, the more stored elastic energy remains, the more supersaturation state exists to enhance the hydrogen flux. The new proposed mechanism explains the shape of hydrogen permeability curves.

3) The amount of microvoids in steel does not have a strong effect on hydrogen diffusion.

4) As the density of dislocation increases in steel induced by cold rolling, the hydrogen diffusion coefficient is decreased while the hydrogen concentration in a steel substrate is increased. Finally, the hydrogen flux increases small amounts with dislocations.

5) Surface roughness does not have any influence on hydrogen diffusion coefficient. The hydrogen concentration increases up to a certain roughness, then decreases according to the variation of the surface energy on the steel substrate. Therefore, the hydrogen flux shows the maximum value for a certain value of surface roughness.

6) The passive layer, such as Fe oxide or Fe hydroxide, if formed on the steel surface, reduces significantly the hydrogen diffusion coefficient. But no effect on the hydrogen concentration was found. Therefore, the decrease of the hydrogen flux by the passive layer results solely from the decrease of the hydrogen diffusion coefficient.

7) The Pd coating reduces the hydrogen flux in steel. It does not, however, give any significant effect on the hydrogen diffusion coefficient. In addition, it removes the effect of surface roughness on steel substrate effectively. A β-Pd hydride and a passive layer can be formed under high concentration of hydrogen environment and these delay the hydrogen diffusion too.

8) On the basis of the results of this study, suggestions and comments were offered to the industry. These recommendations can be used to reduce the surface defects observed in the enamel coating.

REFERENCES

1. Denny A. Jones, Principles and Prevention of Corrosion, Prentice Hall Inc., New Jersey, U.S.A., 1992
2. Gerard Beranger, Guy Henry and Germain Sanz, The Book of Steel, Intercept Ltd., Andover, UK, pp. 984~993, 1996
3. J. J. DeLuccia, Electrochemical Aspects of Hydrogen in Metals, ASTM Hydrogen Embrittlement, Philadelphia, PA 19103, STP 962, pp. 17~34, 1988
4. C. Wu, W. Norton and A. M. El- Sherik, Metallographic Evaluation of VIT 1 Steels, Dofasco internal report, 1999
5. P. Kedzierzawski, Diffusivity of Hydrogen and Its Isotopes in Iron Alloys, Hydrogen Degradation of Ferrous Alloys, Noyes Publications, New Jersey, U.S.A., pp251~270, 1985
6. M. Smialowski, Hydrogen in Steel, Addison-Wesley Publishing Company Inc., London, UK, 1962
7. J. P. Hirth, Theories of Hydrogen Induced Cracking of Steels, Hydrogen in Metals, American Society for Metals, U.S.A., pp. 5, 7, 36, 1974
8. D. A. Westphal and F. J. Worzala, Hydrogen Attack of Steel, American Society for Metals, U.S.A., pp. 79~89 p, 1974
9. S. Wach, A. P. Miodownik and J. Mackowiak, The Diffusion of Hydrogen through Pure Iron Membranes, Corrosion Science, Vol. 6, pp.271~285, 1966
10. G. M. Pressouyre and I. M. Bernstein, A Quantitative Analysis of Hydrogen Trapping, Metallurgical Transactions A, Vol. 9A, pp. 1571~1580, 1978
11. Wayne. M. Robertson, Measurement and Evaluation of Hydrogen Trapping in Thoria Dispersed Nickel, Metallurgical Transactions A, Vol. 10A, pp. 489~501, 1979
12. R. C. Frank, C. W. Wert and H. K. Birnbaum, Modeling Diffusion through Nonuniform Concentrations of Traps, Metallurgical Transactions A, Vol. 10A, pp. 1627~1630, 1979

13. G. M. Pressouyre, Hydrogen Traps, Repellers, and Obstacles in Steel, Metallurgical Transactions A, Vol. 14A, pp. 2189~2193, 1983
14. J. F. Newman and L. L. Shreir, The Effect of Temperature upon the Solubility and Diffusion Coefficient of Cathodic H_2 in Steel, Corrosion Science, Vol. 11, pp. 25~33, 1971
15. P. Kedzierzawski, Hydrogen Trapping in Iron and Iron Alloys, Hydrogen Degradation of Ferrous Alloys, Noyes Publications, New Jersey, U.S.A., pp. 271~287, 1985
16. J. P. Hirth, Hydrogen-Defect Interactions, Hydrogen Degradation of Ferrous Alloys, Noyes Publications, New Jersey, U.S.A., pp. 131~139, 1985
17. H. H. Johnson, Hydrogen in Iron, Metallurgical Transactions A, Vol. 19A, pp. 2371~2387, 1988
18. A. R. Troiano, General Keynote Lecture, Hydrogen in Metals, American Society for Metals, pp. 3~15, 1974
19. D. P. Smith, Hydrogen in Metals, The University of Chicago Press, Chicago, Illinois, U.S.A., pp. 57, 73, 137, 1948
20. Cailletet, L., Compte Rendu, Vol. 58, pp. 327, 1864
21. Bodenstein, M., Zeitschrift für Electrochemie, Vol. 28, pp. 517, 1922
22. M.A.V. Devanathan and Z. Stachurski, The adsorption and diffusion of electrolytic hydrogen in palladium, Proceedings of the Royal Society of London, Vol. 270, pp. 90~102, 1962
23. M.A.V. Devanathan, Z. Stachurski and W. Beck, A Technique for the Evaluation of Hydrogen Embrittlement Characteristics of Electroplating Baths, Journal of the Electrochemical Society, Vol. 110, No. 8, pp.886~890, 1963
24. M.A.V. Devanathan and Z. Stachurski, The Mechanism of Hydrogen Evolution on Iron in Acid Solutions by Determination of Permeation Rates, Journal of the Electrochemical Society, Vol. 111, No. 5, pp. 619~623, 1964
25. P. Manolatos, J. Le Coze, C. Duret-Thual and M. Jerome, Use of Pure Metals to Analyse Hydrogen Electrochemical Permeation in Steels, Journal de Physique IV, Vol. 5, pp. C7-409~414, 1995

26. P. Manolatos, M. Jerome, C. Duret-Thual and J. Le Coze, The Electrochemical Permeation of Hydrogen in Steels without Palladium Coating. Part I: Interpretation Difficulties, Corrosion Science, Vol. 37, No. 11, pp. 1773~1783, 1995

27. P. Manolatos, C. Duret-Thual, J. Le Coze, M. Jerome and E. Bollinger, The Electrochemical Permeation of Hydrogen in Steels without Palladium Coating. Part II: Study of the Influence of Microstructure on Hydrogen Diffusion, Corrosion Science, Vol. 37, No. 11, pp. 1785~1796, 1995

28. T. Zakroczmski, Entry of Hydrogen into Iron Alloys from the Liquid Phase, Hydrogen Degradation of Ferrous Alloys, Noyes Publications, New Jersey, U.S.A., pp. 215~250, 1985

29. Y. P. Zheng and T. Y. Zhang, Effects of Absorption and Desorption on Hydrogen Permeation, Acta mater., Vol. 46, No. 14, pp. 5035~5043, 1998

30. A. M. Brass and J. R. Collet-Lacoste, On the Mechanism of Hydrogen Permeation in Iron in Alkaline Medium, Acta Mater., Vol. 46, No. 3, pp. 869~879, 1998

31. A. M. Brass, J. Chene and A. Boutry-Forveille, SIMS Analysis of Deuterium Distribution in Palladium Coating on Pure Iron, Corrosion Science, Vol. 36, No. 4, pp. 707~716, 1994

32. S. Wach and A. P. Miodownik, The Diffusion and Permeation of H through Pure Fe Membranes, Corrosion Science, Vol. 6, pp.271~279, 1967

33. Su-il Pyun and R. A. Oriani, The Permeation of Hydrogen through the Passivating Films on Iron and Nickel, Corrosion Science, Vol. 29, No. 5, pp. 485~496, 1989

34. H. G. Ellerbrock, G. Vibrans and H. P. Stuwe, Diffusion of Hydrogen in Iron with Cavities, Acta Metallurgica, Vol. 20, pp. 53~60, 1972

35. Metals Handbook Ninth Edition, Vol. 13, Corrosion, pp. 167

36. G. M. Evans and E. C. Rollason, Journal of Iron Steel Inst., Vol. 207, pp. 1484, 1969

37. Kumnick and H. H. Johnson, Deep Trapping states for Hydrogen in Deformed Iron, Acta Metallurgica, Vol. 28, pp. 33~39, 1980

38. J. P. Hirth and G. J. Dienes, On the Rate of Equlibration of Diffusional Traps in Solids, Acta Metallurgica, Vol. 30, pp. 2061~2064, 1982

39. T. K. Govindan Namboodhiri and L. Nanis, Concentration Dependence of Hydrogen Diffusion in Armco Iron, Acta Metallurgica, Vol. 21, pp. 663~672, 1973

40. C. Wu, Characterization of Void Structure for VIT Material CC 075-0.043" Gauge, Dofasco internal report, 1999

41. A. M. Pritchard and B. T. Mould, Mössbauer Spectra of some Iron Compounds formed from Alkaline Solutions, Corrosion Science, Vol. 11, pp. 1~9, 1971

42. Norio Sato and Morris Cohen, The Kinetics of Anodic Oxidation of Iron in Neutral Solution, Journal of the Electrochemical Society, Vol. 111, No. 5, pp. 512~522, 1964

43. D. D. Macdonald, The Electrolyte-Iron Interface, Hydrogen Degradation of Ferrous Alloys, Noyes Publications, New Jersey, U.S.A., pp. 78~113, 1985

44. Masaichi Nagayama and Moris Cohen, The Anodic Oxidation of Iron in a Neutral Solution, Journal of the Electrochemical Society, Vol. 109, No. 9, pp. 781~790, 1962

45. J. O'M. Bockris, J. McBreen and L. Nanis, The Hydrogen Evolution Kinetics and Hydrogen Entry into α-Iron, Journal of the Electrochemical Society, Vol. 112, No. 10, pp. 1025~1031, 1965